

POLITECNICO DI TORINO

**Department of Engineering
Master Degree in Electronic Engineering**



**Micro Supercapacitor:
fabrication and characterization of an
asymmetric device in aqueous electrolyte**

Supervisor

Prof. Andrea LAMBERTI

Candidate

Mariacristina CASASCO

October 2021

Summary

The dream for an energy storage device is have an high energy density together with an high power density. The capacitors and the batteries try to improve at the maximum one of these two quality, but the trade-off can be found thanks to the supercapacitors. These new devices are similar to a capacitors, but instead to have a dielectric between the two electrodes they have an electrolyte: the charge storage is possible thanks two different phenomena, the electrical double layer and the pseudo-capacitance. The field of application is increasing: they could be used as capacitors when an high power density is needed, however having an high capacitance they could be also integrated with other devices similarly to batteries. This latter characteristic could be helped also with the scaling down of the dimensions creating micro-supercapacitors and the aim of the thesis is try to physically create its. These devices are small and so can easily integrated with other electronic devices, increasing the field of applications.

The state of the art moves towards higher performance devices, but at the same time could be useful study low cost, health safe and environmentally friendly's processes and devices.

The project starts with the idea of creating wearable devices and for this is chosen a flexible Kapton substrate for the electrodes. Then, these are covered before by thin films, after that, an electrochemical deposition of porous 3D gold is carried out to increase the superficial area, and after they are covered with active materials to increase the capacitance exploiting the EDLC and pseudo-capacitance. To increase the power and the energy density, the potential window is risen creating asymmetric devices: one electrode consists of activated carbons exploiting the effect of the electrical double layer, instead the second one is formed by manganese oxide taking advantage from the pseudo-capacitance. The deposition techniques are studied setting different parameters to find the best result. For the gold deposition first is used the evaporation process to create an adhesion layer of chromium and gold and then is applied the electro-plating process to create the dendritic gold. Also the manganese oxide is placed thanks an electro chemical process, instead the

carbon particles are fixed with an electro-phoretic deposition.

The family of possible electrolyte is very big, but by targeting the cost, health safe and environmentally friendly the neutral electrolyte Na_2SO_4 is chosen. The interaction between this and the electrodes' materials is studied, characterising them and trying to create devices with optimized performance. In fact, typically the aqueous electrolytes have a limited potential window due to the electrolysis effect of the water at 1.23 V, but creating asymmetric devices is possible increase it up to 1.6 V.

Different kind of SCs' configuration are analysed, from the stack, where the two electrodes are one in front to the other, to the planar in which the two are in the same plane. About this last layout is possible try to increase the capacitance creating also interdigitated devices.

Furthermore, the use of photolithographic process permits a distance of some hundred of micrometres about the two electrodes, creating micro-super-capacitors.

Finally planar geometries begin to be analysed trying to find the best trade off with the optimization of the capacitance and the physical fabrication, leaving space for further developments.

Acknowledgements

Alla mia famiglia, i miei fan numero uno, per credere sempre in me prima ancora che lo faccia io.

Al professor Andrea Lamberti, relatore ed ideatore di questa tesi, per la disponibilità e i consigli.

Allo studente di dottorato Davide Arcoraci, tutor in questo progetto, per la pazienza e l'aiuto senza i quali questa tesi non sarebbe stata possibile.

Al dottor Pietro Zaccagnini, co-tutor di questo progetto, per l'interessamento e la passione che mette in tutte le attività di ricerca del DISAT.

Ai miei amici, quelli con cui ho condiviso ogni step di questo percorso e non solo, per esserci ed esserci stati davvero sempre.

E infine al gruppo di ricerca del DISAT, le persone con cui ho trascorso la maggior parte del tempo negli ultimi mesi, per avermi subito accolta nel loro gruppo e per avermi fatto trascorre un periodo semplicemente fantastico.

Table of Contents

List of Tables	VIII
List of Figures	IX
Acronyms	XVII
1 Introduction	1
1.1 Super Capacitor	1
1.2 State of the art	5
1.3 Aim of the thesis	7
1.4 Organization of the thesis	7
2 Characterization of the current collector materials	9
2.1 Electrodes' measurement	9
2.1.1 Three electrodes measurement	11
2.1.2 Two electrodes measurement	13
2.2 Electrochemical characterization techniques	14
2.2.1 CV: Cycling Voltammetry	14
2.2.2 EIS: Electrical Impedance Spectroscopy	15
2.2.3 CCDC: Constant Current Charge and Discharge	19
2.3 Electrolyte	21
2.4 Current collector	24
2.4.1 Substrate	24
2.4.2 Electroplating of the gold	24
2.4.3 Characterization of the current collector material	29
3 MnO₂ Electrode	37
3.1 Electroplating deposition	37
3.1.1 Set-up	37
3.1.2 Characterization	39

4	Carbon-based electrode	45
4.1	EFD: Electro Phoretic Deposition	45
4.1.1	Colloidal solution	45
4.1.2	Set-up	47
4.1.3	Characterization	50
5	Asymmetric stack device	57
5.1	Realization of an asymmetric device	57
5.2	Measure's results	58
6	Planar device	63
6.1	Introduction	63
6.2	Photolithographic process	63
6.3	Characterization of each electrode	65
6.4	Creation of the device	67
6.4.1	Results	67
7	Conclusions and future developments	70
7.1	Conclusions	70
7.2	Future developments	71
7.2.1	Deposition techniques	71
7.2.2	Stack device	72
7.2.3	Planar device	72
	Bibliography	73

List of Tables

2.1	Comparison of the density of capacitance, 'C', evaluated with the CV and the equivalent series resistance 'ESR', evaluated with the EIS, of the two deposited gold types. The 3D gold have better parameters with respect to the planar gold. The sample has an area of 1 cm^2	36
3.1	Comparison of the density of capacitance, 'C', evaluated with the CV and the equivalent series resistance 'ESR', evaluated with the EIS, of the planar gold and manganese dioxide. The difference in capacitance is of a factor 69.	42
4.1	Comparison of the density of capacitance, 'C', evaluated with the CV and the equivalent series resistance 'ESR', evaluated with the EIS, of the two deposition methods. The Electro-phoretic-deposition have better parameters with respect to the precipitation methods. .	54
4.2	Comparison of the density of capacitance, 'C', and equivalent series resistance 'ESR', of the three carbon based-materials. The capacitance is obtained with a CV, instead the ESR with an EIS. The ball-milling AC have the best performance between the three. . . .	56
4.3	Comparison of the density of capacitance, 'C', and Coulombic efficiency ' η ', of the CB and MnO_2 at +0.4 V. How it is possible see, the MnO_2 is the best between the two.	56
6.1	Comparison of the density of capacitance, 'C', and Coulombic efficiency ' η ', of the two tested planar devices, one digit and planar, with the stack device.	68

List of Figures

1.1	Ragone Plot [2]. It shows the difference performance evaluations of the storage energy's devices, comparing the energy density (vertical axis) with respect to the power density (horizontal axis).	2
1.2	Representation of IHL and OHL [5]. It shows how molecules adsorbed form IHL, while solvated ions create OHL. The polarised electrode and the ions in the electrolyte create two layers that could be seen as two parallel electrodes in a capacitor, placed at a very small distance depending on the size of the solvent's molecules.	4
2.1	Equivalent circuit representation of the interface electrode-electrolyte according to the Randles' circuit. The 'C' is the capacitance of the EDL, the 'Z' is a parallel impedance that represents the Faradaic reactions that can occur instead the 'Rs' is a series resistance due by the electrolyte.	10
2.2	Equivalent circuit representation of a SC. The two series blocks of 'C' and 'Z' represent the two interfaces electrode-electrolyte, one for each electrode. The electrolyte is seen as a resistance 'Rel' instead the two contacts have each a resistance 'Rc'.	10
2.3	Equivalent circuit representation of the series of the working and the reference electrode. On the left, there is the interface electrode-electrolyte, in the middle, the resistance of the electrolyte while on the right the reference electrode. The voltage drop across the reference electrode is constant and so, applying a voltage to all the system, is possible understand how much is the drop across the interface.	12

2.4	Comparisons between different CV of different devices. On the vertical axis is present the current, instead on the horizontal axis there is the voltage applied. In green, is possible see the behaviour of an ideal capacitor. In red, the behaviour of a capacitor with a resistive component and in black the behaviour of a pseudo SC. On the left of this latter curve is present a peak typical of a reaction present in the pseudo-capacitor.	15
2.5	On the left simply representation of an EDLC consisting by the series of the resistance ESR, ' R_s ', and the capacitance of the EDL, ' C_{dl} '. On the right the correspondingly Nyquist plot [5].	17
2.6	On the left simply representation of an EDLC consisting by the series of the resistance ESR, ' R_s ', the capacitance of the EDL, ' C ' with the adding of a diffusive element ' Z_W '. On the right the correspondingly Nyquist plot where ' Ω ' represents the electrolyte resistance within the pores [5].	18
2.7	On the left, complete representation of an pseudo-capacitance consisting by a resistance ' R_s ', contact and internal resistance, a capacitance ' C_{dl} ' of the EDL, in parallel to the faradaic impedance. The latter consists of a faradaic resistance ' R_F ' in series to the faradaic capacitance ' C_Φ '. On the right the correspondingly Nyquist plot [5].	18
2.8	CCDC result. On the left y-axis, the voltage recorded over time is present, on the right y-axis the applied current over time. The voltage presents a drop in the peak called IR drop [3].	20
2.9	Pourbaix's diagram of the gold. On the y-axis are present the reduction potentials. On the x-axis is present the pH of the electrolyte solution. In the plot are present different zones: in each zone is written the type of material that is created under that voltage and pH solution [17].	22
2.10	CV comparison between bulk gold in Na_2SO_4 1M and KOH 1M. The CV is set into a open cell with 50 ml of solution and using as reference the Ag AgCl 3M in KCl of the Metrohm. The counter electrode is a platinum wire and the scan rate is set at 1mV/s. How it is possible see, the two CV are very similar, only shifted due to the different pH of the electrolyte.	22
2.11	Potential measurement of the Ag AgCl wire in 1M Na_2SO_4 refereed by the Ag AgCl of the Metrohm company in 3M of KCl. This potential is monitored for 24 hours that are 86400 s.	23

2.12	Electroplating deposition. On the left, electrodes of 50 μm of titanium after a gold electro-plating. The electrode number '1' is fabricated with a current density of 0.5 mA/cm^2 , the number '2' with 0.6 mA/cm^2 and so on, until the number '21' fabricated by a current density of 2.5 mA/cm^2 . The other parameters like temperature, distance and time are fixed. On the right, a photo of the set-up where is possible see the sacrificial layer on the right and the sample on the left.	26
2.13	Calibration curve for bulk electroplating process. On the y-axis is present the density of mass deposited with a specific current density indicated on the x-axis. The points from the left to the right are correspondingly to the electrode '1', '2', '3'...'21' shown in the figure 2.12.	27
2.14	Voltage recorded during the electroplating deposition of gold at 1.5 mA/cm^2 . How it is possible see the voltage stabilises at 0.7 V for a small time and then increases up to 1.15V. Exactly after this point, the deposition passes from planar to dendritic.	28
2.15	3D gold deposition. On the left a visual comparison between planar (yellow) and 3D gold (brown). On the right a Fesem image of dendritic gold deposition. The dendrites have an height of some micrometers and is possible see the porosity and the increase of the area that they introduce.	29
2.16	EIS of a bulk electrode of gold in 1M Na_2SO_4 . Above there is the Nyquist plot: the ESR is low, but being an open cell it depends by the distance between the reference and the sample. Under there is the Bode plot: the phase is about 80° and decreases a bit at low frequency.	30
2.17	CV of a bulk electrode of gold in 1M Na_2SO_4 , blue line. The window is from -1.4 V to +1.5 V. To do a comparison is shown also the CV of a bulk electrode of which are grown 3D structures, in red. The reactions are the same, but the magnitude of the 3D is bigger. . . .	31
2.18	EIS of a bulk electrode of titanium on which is plating the dendritic gold. Above there is the Nyquist plot, on the left a full scale view, on the right a zoom: the slope is good and the ESR is of 0.82 Ω . Under there is the Bode plot: the phase is about 80° and remains constant also for low frequency.	32
2.19	CV and Coulombic Efficiency of a bulk electrode of titanium on which is plating the 3D gold. Superposition of the anodic potential windows and the cathodic potential windows.	33

2.20	EIS Nyquist comparison of the planar gold, blue line, and the 3D gold, red line. On the left there is a full axis view, on the right a zoom. The range of frequency is from 1 MHz to 10 mHz.	35
2.21	CV comparison between the planar gold, blue line, and 3D gold, red line. The scan rate is set at 5 mV/s and for each the number of scans is 30.	35
2.22	CV of planar gold, blue line, for the anodic window. The scan rate is 5 mV/s and for each CV the number of scans is 30.	36
3.1	Voltage measured during the electroplating deposition. The current density is set at -1 mA/cm^2 where the working electrode ('+') is put on the sample. The area under test is of 1 cm^2	38
3.2	Manganese dioxide deposition. On the left the comparison between the planar gold with and without the manganese dioxide above. The first is before the calcination, the second after. On the right the two electrodes set-up for the electroplating deposition of manganese dioxide. In the latter, on the right there is the working electrode on which is applied a current density of -1 mA/cm^2 with respect to the counter electrode on the left. This set-up is only used to save quantity of electrolyte and is used only after the characterization at three electrodes.	39
3.3	EIS graphs results. Above there is the Nyquist plot: the two images are the same, the left is with the full axis, the right is a zoom at high frequency. Above the correspondingly Bode plot.	40
3.4	CV curve on the overall voltage window, from -0.9V to 0.9V . The used scan rate is of 5 mV/s and for each cycle the number of scans is of 20. The area of the tested electrode is of 1 cm^2	41
3.5	Superposition of different cycles of CV, from $+0.1 \text{ V}$ to $+1.3 \text{ V}$, with the correspondingly Coulombic efficiency η . The used scan rate is of 5 mV/s and for each cycle the number of scans is of 20. The area of the tested electrode is of 1 cm^2	41
3.6	Comparison between the gold, red line, and the manganese dioxide, blue line. Above an EIS where is possible see how much the imaginary part of the two are different. At the bottom the superposition of different CV. Of course is possible see the visual difference between the two levels of current and so the big difference in term of capacitance. The two are both obtained with a scan rate of 5 mV/s and are the result of 30 scans, both with an area of 1 cm^2 . The only difference is OCP value starting point that is different for the two materials. The difference about the two values of capacitance is about a factor 69.	43

3.7	FESEM image comparison between planar gold and manganese dioxide. Above is present the MnO_2 and below the planar gold. . .	44
4.1	EFD vertically set-up. On the left the result, comparing the electrode before and after the deposition, on the right the correspond set-up. In this latter, on the left is shown how to put the working electrode (yellow) and the platinum counter electrode (grey) into the colloidal solution (black). Between these is applied a voltage so that the electrode in which there is wanted the deposition is positive charged. On the right is shown an example of how the electrode will be. The deposition is not uniform and so, in the under part, the carbons are more present (more black color).	48
4.2	EFD horizontal set-up. Above is shown how to put the working electrode (yellow) and the titanium counter electrode (grey) into the colloidal solution (black). Between these, is applied a voltage so that the electrode in which there is wanted the deposition is positive charged. On the bottom is shown an example of how the electrode will be. The deposition is more uniform (black color), but the red arrow indicates the critical point at which happens the delamination.	49
4.3	Photo of the set-up for the EFD. In the foreground is present the sample between which is applied a field. In the background, on the left an amperometer to measure the current, on the right a voltage source to generate a voltage.	50
4.4	Superposition of different cycles of CV, from -0.1 V to -1.2 V, with the correspondingly Coulombic efficiency η . The used scan rate is of 5 mV/s and for each cycle the number of scans is of 20. The area of the tested electrode is of 1 cm^2	51
4.5	Superposition of different cycles of CV, from -0.9 V to -1.2 V, with the correspondingly Coulombic efficiency η . The used scan rate is of 5 mV/s and for each cycle the number of scans is of 30.	52
4.6	CV comparison of the carbons black, blue line, with respect to the 3D gold, red line. The area is for both at 1 cm^2 , while the scan rate is of 5 mV/s.	52
4.7	EIS comparison between the CB applied with a voltage, blue line, and without, red line. The two plots are the same: on the left there are the line correspondingly to all the frequency, from 10 mHz to 1 MHz, instead on the right there is a zoom of the higher frequency. The area of all the tested electrodes is of 1 cm^2	53
4.8	CV comparison between the CB applied with a voltage, blue line, and without, red line. The application of a voltage is of -1 V for the both and the used scan rate is of 5 mV/s.	53

4.9	EIS comparison between the carbons black 'CB', blue line, the activated carbons obtained with the Ball-Milling 'AC BM', green line, and without the Ball-Milling 'AC', red line. The two plots are the same: on the left there are the line correspondingly to all the frequency, from 10 mHz to 1 MHz, instead on the right there is a zoom of the higher frequency.	55
4.10	CV comparison between the CB, AC BM and AC. The application of voltage is of -1 V for the both and the used scan rate is of 5 mV/s.	55
5.1	Superposition of the anodic CV, with the MnO_2 , and the cathodic CV, with the CB, in blue. The red line shows the Coulombic efficiency correspondingly at the voltage windows. The dot green line is set at 97 % for the anodic, and at 99% for the cathodic. . .	58
5.2	EIS graphs results of an asymmetric stack device. Above there is the Nyquist plot: the two images are the same, the left is with the full axis, the right is a zoom at high frequency. Above the correspondingly Bode plot.	59
5.3	CV of asymmetric stack device consisted of an anode electrode of MnO_2 and a cathode electrode of CB. The ratio between the two areas is of 1.6, the first has an area of 1 cm^2 the second of 1.6 cm^2 . The used scan rate is of 5 mV/s and the scans are of 30.	60
5.4	Rate capability plot. On the y axis is present the density of capacitance instead on the x axis is present the number of cycles. In this figure are cut the ranges in which the device doesn't work.	61
5.5	GCD profile refereed to three different range of current. Increasing the range is possible see that the IR drop increases.	61
5.6	Ragone plot. On the y-axis is the energy density and on the x-axis is the power density. Above are shown the experimental results of the asymmetrical device. Below are references to the literature where the green pentagon represents the tested device [26].	62
6.1	Example of two masks produced for the creation of planar devices. The devices are in the middle, instead in the corners there are examples of layouts used for the measure of the sheet resistance, used for the evaluations of the thickness of the substrate.	64
6.2	Set-up of the photolithographic process with the UV source, into a class 100 clean-room.	65

6.3	Different set-up for a three electrodes measurement. On the left there is a stack configurations where the working electrode (WE), the reference (REF) and the counter electrode (CE) are put one each above the other because the reference is a wire so is possible. On the right instead a planar configuration where the reference and the electrode are in the same plane and above are put the fiber glass with the counter-electrode.	66
6.4	Planar device results. On the left is possible see the manganese dioxide, while on the right there is the carbons black particles. The two electrodes have a distance of $300\mu m$	68
6.5	Planar device and stack comparison results. Above there is the EIS and below the CV comparison. The blue line represents the stack device with an area of 1.6 cm^2 , the green line the two rectangular electrodes planar put in a distance of 300 cm^2 and with an area of 1.54 cm^2 , while the red is the planar one digit with an overall area of 0.87 cm^2 and which electrodes are separated of $100\ \mu m$ of distance.	69

Acronyms

AC

Activated Carbons

BM

Ball Milling

CB

Carbons Black

CV

Cycling Voltammetry

CCCD

Constant Current Charge Discharge

EDL

Electrical Double Layer

EDLCs

Electrical Double Layer Capacitors

EFD

Electro Phoretic Deposition

EIS

Electrical Impedance Spectroscopy

ESR

Equivalent Series Resistance

IHL

Inner Helmholtz Layer

IR

Internal Resistance

OCP

Open Circuit Potential

OHL

Outer Helmholtz Layer

SCs

Super Capacitors

Chapter 1

Introduction

1.1 Super Capacitor

Overview

A super-capacitor (SC), also called electrochemical capacitor or ultra-capacitor, is an energy storage device like an electrolytic capacitor and a battery.

To understand the difference between them could be useful compare the energy density, that is the amount of energy that could be stored, and the power density that denotes how quickly this amount of energy could be released. The batteries have an high energy density instead the electrolytic capacitor an high power density. The Ragone plot (fig 1.1) is a Cartesian plane where these two quantities, the energy and power, are shown normalized with respect to the mass of the device respectively on the vertical and horizontal axis [1]. How it is possible see, the SCs are between the two devices: as capacitors they have an high power density but they try to improve the energy density like the battery.

This behaviour allows them to overcome the limits of the other devices, covering applications impossible for them. In fact, thanks to these advantages, the SC can be used in applications where fast and numerous charging cycles are required. For example in the electrical vehicles in the city where stopping and starting occur many times or in portable consumer electronics [3] for the materials with which they are fabricated, but also military, industry and memory systems are applications field [3] under study.

Thanks to the storage's principle of energy, that will be explained next, the SCs have advantages also in high cycling life and low production of heat [3].

Moreover these SCs can be scaled down, improving the integration with other electronic components increasing the field of applications. With this idea was born the Micro Super Capacitors. The term "Micro" means that one dimension of the device has micro metric size, like for instance the distance between the

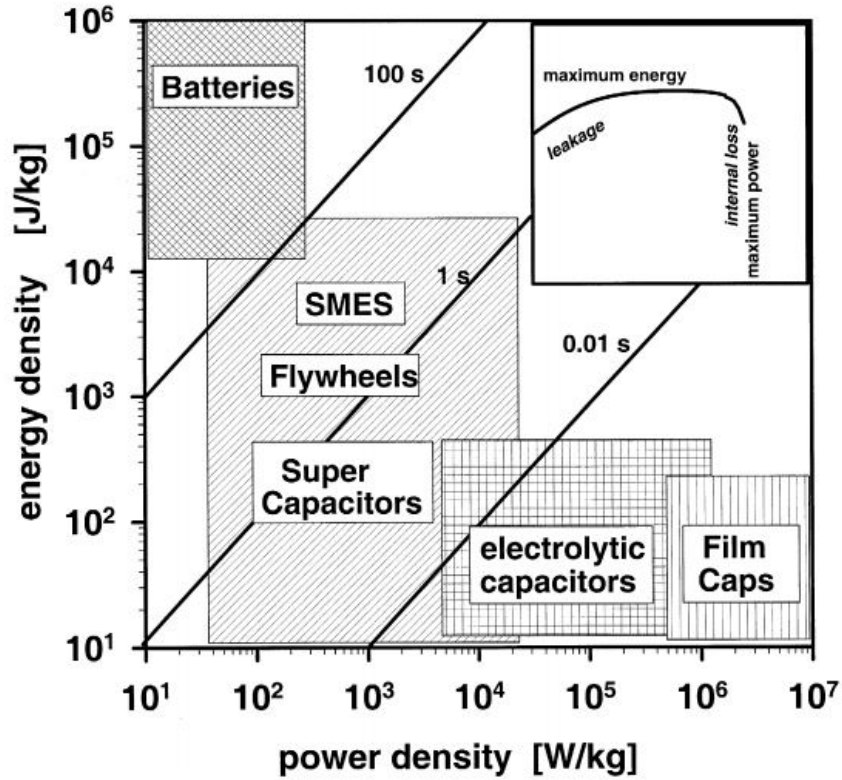


Figure 1.1: Ragone Plot [2]. It shows the difference performance evaluations of the storage energy's devices, comparing the energy density (vertical axis) with respect to the power density (horizontal axis).

two electrodes. Instead the term "integration" means that the μSCs can be put together with other electronic components.

The advantages of the SC come from the energy storage mechanism, which is different from a normal capacitor. In a parallel-plate capacitor, the charge is achieved by the physical separation from a dielectric of two electrodes, between which a voltage is applied. This is true for the solid dielectric, but also in the electrolytic capacitor this characteristic is present because the dielectric is obtained by oxidation of an electrode. In these devices the capacitance can be evaluated as expressed in the equation 1.1:

$$C = \epsilon \cdot \frac{A}{d} \quad (1.1)$$

where ' ϵ ' is the dielectric constant of the dielectric, ' A ' is the area of the electrode

and ' d ' is the distance between two electrodes.

The SCs have a different operating principle. Although the two electrodes are always separated by a physical separator and the capacitance is always proportional by the area and by the distance as in the equation 1.1, in the SCs there is not a dielectric. Instead, there is an electrolyte that fills and can easily pass through the separator between the two electrodes. In this set-up the storage of energy is possible thanks to two different principles that generate three different families of SCs:

- EDLCs (Electrical Double Layer Capacitors): these devices operate on the principle of the electric double layer (EDL) in which there is a build-up of electrostatic charge.
- Pseudo-Capacitors: these devices operate with an electrochemical charge storage.
- Hybrids Capacitors: these devices use both the EDL and the pseudo-capacity principle as charge storage.

Electrical Double Layer Capacitors (EDLCs)

In EDLCs, charge storage occurs electrostatically, i.e. without chemical reactions between the electrodes and the electrolyte.

This absence of reactions permits a low heat generation and an high cycling life that are two big advantages of the SCs. The operating principle that makes this possible is the creation of a double layer of opposing ions across each electrode.

When a voltage is applied to an electrode, oppositely charged ions in the electrolyte are attracted. These two layers of opposite charges, placed opposite each other, can be seen as parallel electrodes of a capacitor where charge can be stored [4].

This simple representation of the phenomena was introduced the first time by the physics Hermann von Helmholtz, however a better description of the phenomena is present in the Grahame model.

The electrolyte is a solution in which a process of solvation is present: solute's molecules are surrounded by solvent's molecules. When an electrode is polarised, it begins to attract the solvated molecules, and when these reach the surface, the solvent's molecules are physically adsorbed by the electrode. This means that the cations or anions, depending on the polarisation of the electrode, of the electrolyte are not directly in contact with the electrode, but are at a distance which depends on the size of the solvent's molecules surrounding it. This distance is called the outer Helmholtz layer (OHL) and is about the size of a solvent's molecule, so it is very small. Recalling that the capacitance is inversely proportional to distance (equation 1.1), this explains why the device in which this phenomenon occurs could be called a super-capacitor. A graphical representation of this can be seen in the

figure (1.2), where together with the OHL the inner Helmholtz layer (IHL) is also shown, which is formed simply by the solvent's molecules.

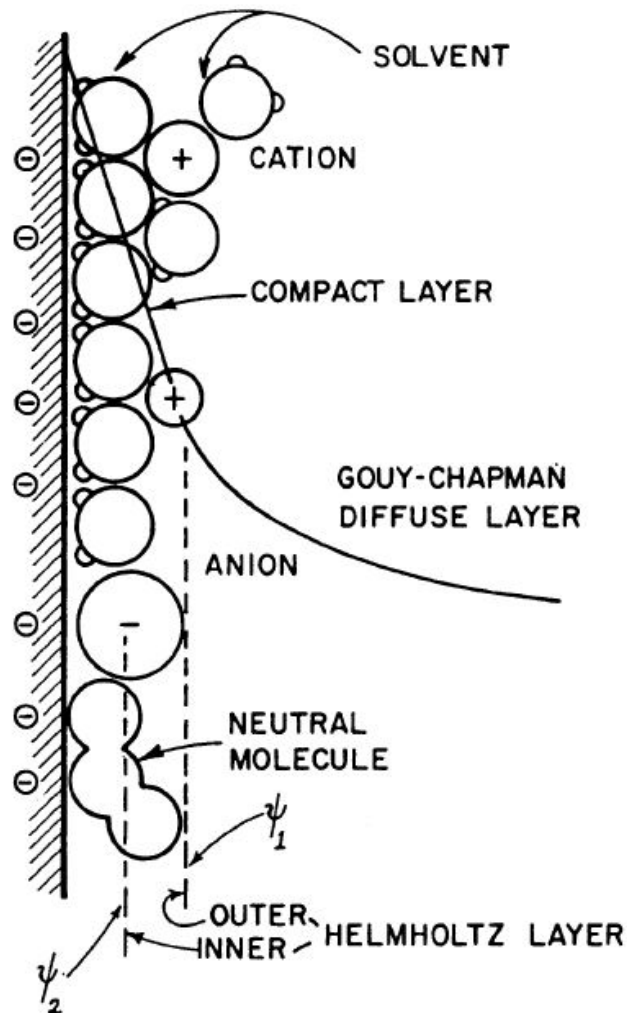


Figure 1.2: Representation of IHL and OHL [5]. It shows how molecules adsorbed form IHL, while solvated ions create OHL. The polarised electrode and the ions in the electrolyte create two layers that could be seen as two parallel electrodes in a capacitor, placed at a very small distance depending on the size of the solvent's molecules.

These layers put in front of the electrode form the "compact layer" described by Helmholtz, that explains the capacitive propriety. In theory these layers should perfectly balance the charge in the electrodes, but thanks to the thermal fluctuation

due to the Boltzmann principle, the molecules are not fixed and so the perfect balance is not achieved. This means that behind the "compact layer", there are other ions that are attracted by the field in a softer mode. This second zone is called Gouy-Chapman diffuse layer, in honor of the scientists who preached it, and here the voltage drop is exponential decreasing with the distance [5].

Pseudo-Capacitors

In the Pseudo-Capacitors the store of energy is faradaically. When one electrode is polarized, it begins to attract the ions of the electrolyte. Typically these ions are solvated so they don't come in direct contact with the surface of the electrode forming the EDLCs. However if some of these are desolvated, when they reach the surface they start to create bonds where the energy is stored.

The reactions due to this phenomena are of the kind red-ox, so between the surface of the electrode and the ions of the electrolyte there is only a passage of electrons. From an electrical point of view it means that there is a current flowing through the device: for this in the capacitors is said that the energy is stored faradaically. Unlike the battery, this process don't create chemical bonds creating new substance, but there is only a passage of the electrons so it explains why the cycling life is higher in the SC than in the battery. Moreover these devices have a better energy density than the EDLCs because is possible store more energy in the bonds, but have a lower power density [6] because more time is needed to release this energy.

Hybrids Capacitors

The Hybrids Capacitors are a trade-off between the EDLCs and the Psuedo-Capacitors. In this both the effects of the electrical double layer and psuedo-capacitance are equal present [6].

1.2 State of the art

The SCs are composed by two electrodes separated by a physical separator filled by an electrolyte. Both for the EDLCs and the pseudo-capacitors the aim of the future development is increase the capacitance, so the energy density, trying to not loss in power density.

According to the equation 1.1 increasing the surface area the capacitance increases. Fixing a final physical dimension, the increase of the surface area can be obtained using materials with high porosity. The carbon-based materials are a very common choice for the EDLC's electrodes, thanks to their high porosity and low cost of production [3]. For the pseudo-capacitors instead, the metal oxide as RuO_2 and

Fe_3O_4 are typically used [7], but also the MnO_2 is has been very well researched [8].

However high porosity not always means high capacitance. In fact the surface area can increase, but is necessary a correct match between the size of the pores and the size of the ions of the electrolyte to obtain an high capacitance [3]. This means that is important find the right electrolyte for the right electrode's material.

The electrolyte plays an important role also in the selection of the operating potential window that is the voltage that can be applied between the two electrodes. Try to increase it, is very important, because the energy density expressed in the equation 1.2:

$$E = \frac{1}{2} \cdot C \cdot V^2 \quad (1.2)$$

is proportional to the square of the voltage window, so the increase of the voltage window means an increase the energy density and, at the same time, also an increase in the power density. The organic electrolyte was one of the first kind of electrolyte chosen exactly for this characteristic.

Increased performance is, of course, one of the main objectives of future developments, but several trade-offs can be made if the main focus is changed towards production cost, safety or the environmental factor.

Looking towards these latter goals, the study and the use of the aqueous electrolyte is increasing. Compared with respect to the organic electrolyte, the aqueous electrolyte does not pose any problems for people's health, is cheaper, environmentally friendly and also highly conductive. As it will be better explained next, the increase in the conductivity means the decrease of the electrolyte's resistance, enhancing the capacitance effect of the whole device. On the other hand, the greatest limitation of the aqueous electrolyte is the potential window limited to 1.23 V due to the electrolysis of water. This limits the energy and power density compared to an organic electrolyte, that has a potential window above the 2 V [9].

Some solutions can however overcome this limited potential window. In fact is possible create an asymmetric device in which the two electrodes are not equal, but consist of two different materials [10]. For instance, is possible create a super capacitor in which the cathode, the negative electrode, is covered with activated carbons, instead the anode, the positive electrode, is covered with metal oxide, for instance the MnO_2 [11].

The shape also plays an important role: is possible place the electrodes opposite each other or create a planar configuration in which one dimension, the vertical, is completely gained. About the planar device is further possible create different layouts trying to improve the performance.

With regard to the electrodes, there are different deposition techniques depending on the materials and arrangement. The precipitation method could be very easy to implement and could be used when the two electrodes are facing each other.

However, when there is a planar device, it cannot be used because the aim is to deposit the material only on one electrode, not on both. So galvanic methods such as electrodeposition or electrophoresis could be the solution, but the intensity of this current or voltage could destroy the device. Depending on the final goal, there are generally several possibilities regarding the choice of materials, their deposition, the type of electrolyte and the final layout.

1.3 Aim of the thesis

The aim of the project is create an asymmetric micro super capacitor.

The device will work with an aqueous electrolyte and one goal of the thesis is try to increase its limited potential window. To do this will be used carbon based materials for one electrode and the manganese dioxide for the other. Unlike from the literature in which is used the precipitation method [12], in this thesis are used as deposition techniques the electroplating and the electrophoresis, because these can be used also in planar devices.

The high capacitance typical of a super capacitor is achieved by the EDL effect on one electrode and a pseudo-capacitance effect on the other electrode.

The increase in surface area can be further investigated by trying to place an underlying layer of dendritic gold over the electrode with activated carbons.

The future development will be create complex planar devices. However the aim of this thesis is analyse and find techniques, procedures, materials that will make possible this idea, trying to do also some experiments and examples of simply layouts in this direction.

1.4 Organization of the thesis

After a brief overview on the SCs, in the following sections are present the analysis and studies experimentally done on the SC under test of the thesis.

In the chapter 2 is present the characterization of the current collector into the aqueous electrolyte. In this section are present also some references to the measurement's theory that is necessary to know in order to understand the why in some choices.

In the chapter 3 there is the description of the set-up used to create the electrode with manganese dioxide, with the experimental results.

Similarly, in the chapter 4, is present the description of the other electrode, the one with carbon based materials.

The chapter 5 contains a description of an asymmetric stack supercapacitor, which was obtained from the results of the previous sections.

In the chapter 6 there is an overview on the planar devices and their criticalities,

with a simple prototype description.

Finally in the chapter 7 are present the overall conclusions and the future developments.

Chapter 2

Characterization of the current collector materials

The current collector is the basis of the electrode. It consists of a substrate on which are deposited the different materials that will compose the device. Thanks to the application of specific materials on it, it will become an electrode.

To understand what happens, from an electrochemical point of view, at the materials in contact with an electrolyte or when they are crossed by a voltage, there are mainly three different characterization techniques: Cycling Voltammetry (CV), Electrical Impedance Spectroscopy (EIS) and the Constant Current Charge and Discharge (CCCD).

These techniques could be used both for the characterization of the materials and for the characterization of the device, depending on the type of measurement's set-up. In fact, there are two possibilities: three electrodes measurement and two electrodes measurement, both discussed in the following sections.

2.1 Electrodes' measurement

To understand how to do a measurement is necessary first study the equivalent electric circuit of a SC.

When an electrode comes into contact with an electrolyte or when a small voltage is applied between the two, its interface could be represented as shown in the figure 2.1, known as the 'Randles' circuit' [13].

When the electrode is polarized, the counter-ions are attracted at the interface, creating the electrical-double layer represented by the capacitance 'C'. If the voltage increases or same reactions are wanted, the electrode's surface begins to adsorb the ions with a consequent passage of current: the interface can be modeled as impedance 'Z'. Because the super-capacitor consists of two electrodes and not only

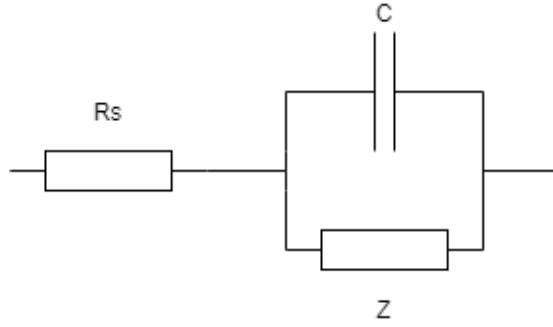


Figure 2.1: Equivalent circuit representation of the interface electrode-electrolyte according to the Randles' circuit. The 'C' is the capacitance of the EDL, the 'Z' is a parallel impedance that represents the Faradaic reactions that can occur instead the 'Rs' is a series resistance due by the electrolyte.

one, is needed to mirror the figure 2.1.

The figure 2.2 shows the equivalent circuit of a SC. The two interfaces are always represented by the parallel of the capacitance and the impedance, as shown in the figure 2.1, but is added the effect of the electrolyte with a resistance R_{EL} and the effect of the contacts with the resistances R_C .

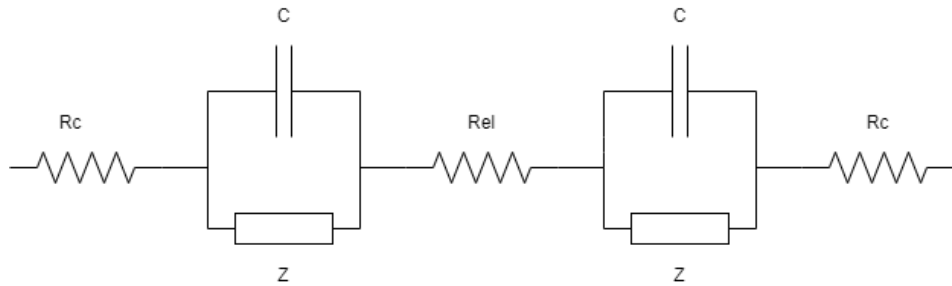


Figure 2.2: Equivalent circuit representation of a SC. The two series blocks of 'C' and 'Z' represent the two interfaces electrode-electrolyte, one for each electrode. The electrolyte is seen as a resistance 'Rel' instead the two contacts have each a resistance 'Rc'.

Is important to notice that the figure 2.2 is true only if the two electrodes are equal, so also the 'C' and the 'Z' are equal. Of course, if the electrodes are different, as in an asymmetric device, each interface electrode-electrolyte will produce a properly capacitance and impedance.

2.1.1 Three electrodes measurement

A solid electrode immersed in an aqueous electrolyte polarises, creating an EDL as shown in the figure 2.1.

This voltage drop present without the application of an external field is called open circuit potential, OCP, and measures the potential that this material has in the electrolyte with respect to a reference.

As this phenomenon occurs independently of the application of an external field, there may be problems during measurement.

To measure this potential is in fact necessary put in parallel at the interface a voltmeter: one probe of the instrument is connected to the electrode and the other at the electrolyte. The first can be modelled as a contact resistance instead the latter by another EDL being a solid electrode into a liquid electrolyte. The problem is that the instrument reads the sum of these two voltage drops, but you don't know how much is one and how much is the other.

A similar situation happens also in the SCs.

The figure 2.2 shows that when a voltage is applied to the SC, it is applied to the series of the two electrode-electrolyte interfaces: if the two electrodes are equal, it can be assumed that the voltage drop is divided into two, but if the device is asymmetric, the voltage drop at each interface is unknown. For the characterization of the SC this could be a problem and for this reason is first necessary characterize the electrode with a specific measurement: the three electrodes measurement.

In a three electrodes measurement, only the voltage drop across an interface is measured. To do this, a voltmeter is put in parallel at the interface with a probe put into the electrolyte. The difference is that this probe, called reference electrode, has, in specific electrolyte, a fixed and known voltage drop. Subtracting by the voltmeter's reading this fixed drop, is possible know the potential that drops across the interface. The scheme shown in the figure 2.3 could clarify this.

To be precise from the figure 2.3 is possible see that also the voltage drop across the electrolyte is unknown because is unknown the resistance 'Rel'. However this resistance can be minimized putting the reference very near to the electrode, so that the voltage drop can be neglected.

This type of configuration works very well only when a small current crosses the system so that the voltage of the reference remains constant during the time. In fact, the reference can be seen as in the figure 2.1, so with a parallel impedance: the increase of the current leads an increase of the voltage drop on it. The result is that it no longer works as a reference. For this is necessary introduce a third electrode called counter electrode. The aim of this, is take the current so that the reference can keep a constant voltage. This ability increases with the increase of the area and, for this reason, the counter electrode consists of materials with high superficial area, like for instance the carbon-based materials.

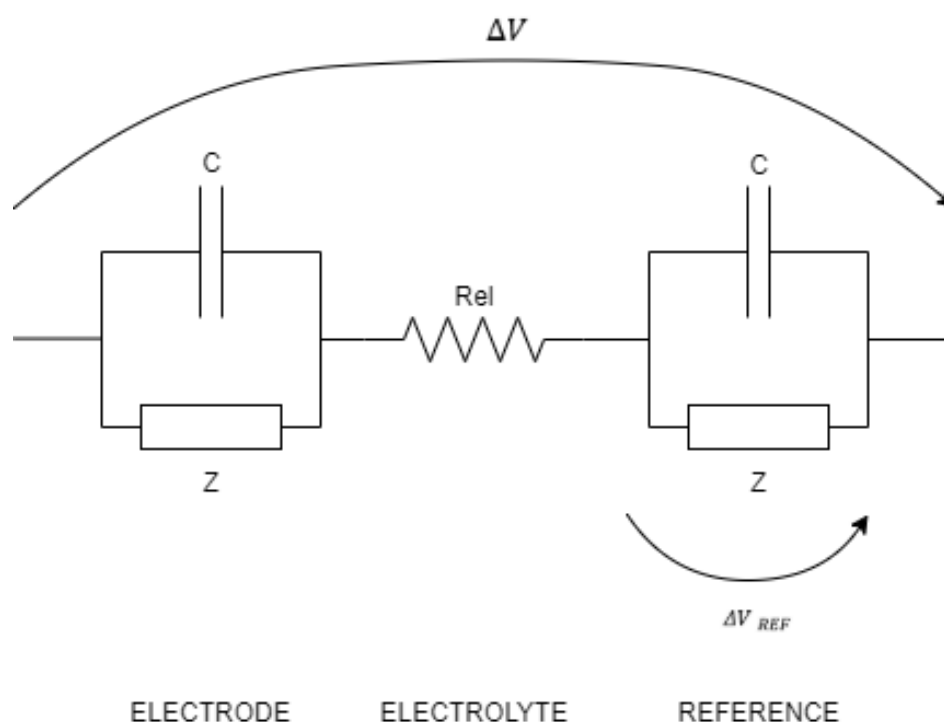


Figure 2.3: Equivalent circuit representation of the series of the working and the reference electrode. On the left, there is the interface electrode-electrolyte, in the middle, the resistance of the electrolyte while on the right the reference electrode. The voltage drop across the reference electrode is constant and so, applying a voltage to all the system, is possible understand how much is the drop across the interface.

Overall, the three electrodes measurement is used for the characterization of one electrode into the electrolyte and is made up of:

- Working electrode: is the electrode under test.
- Reference electrode: it the electrode with respect to is measured and is applied a voltage. To properly work is necessary put its very near to the working.
- Counter electrode: takes the current so that the reference can properly work. To do this, it consists of carbon materials, so has an high superficial area.

These three electrodes are physically created in the thesis' work.

Reference electrode's fabrication

One of the most used reference electrode is the Ag|AgCl in chlorine's solutions. This is typically a wire of silver on which is grown a layer of silver chloride thanks to an anodization process. If is put in a solution with chlorine, as HCl, it has a stable potential, so it can be used as reference electrode.

To create this reference, a wire of silver with a diameter of 0.375 mm is put for 2 h in concentrated ammonia and then all the night in demineralized water for the cleaning. After, the anodization process of the wire is carried in a 0.1 M of HCl applying a current of 0.5 mA/cm^2 for 1 h using as counter electrode a platinum counter electrode.

This reference is preserved holding in 0.1 M of HCl [14].

Counter electrode's fabrication

The counter electrode need to have an high superficial area so it consists of carbon-based materials.

The fabrication process starts with the creation of a solution, then the solvent is evaporated creating a solid structure. The solute consists of:

- 85 % w/w of activated carbons Kuraray YP-50F
- 10 % w/w of carbons black C65
- 5 % w/w of PTFE (Politetrafluoroetilene)

After is added as solvent the ethanol, putting 5 ml of it for each gram of solute. The slurry is then mixed on a stirrer at 60° C until the ethanol has almost evaporated. The material is thus moulded into the preferred shape, and placed in an oven for a day at 60° C to allow the solvent to evaporate completely.

2.1.2 Two electrodes measurement

The two electrodes measurement is used to characterize the device. In fact, once that both the electrodes are characterized, the device can be closed and an overall voltage can be applied between the two electrodes. In this case, the model is shown in the figure 2.2, and thanks to the previous three electrodes measurement, all the voltage drops are known. In this configuration, the reference and the counter electrode are linked together using a single electrode, instead the other electrode is represented by the working electrode. The two electrodes are then connected at the two electrodes of the SC.

2.2 Electrochemical characterization techniques

Both for the three and two electrodes measurement techniques, there are three electrochemical characterization techniques that can be used for the characterization of the SCs: the Cycling Voltammetry (CV), Electrical Impedance Spectroscopy (EIS) and Constant Current Charge and Discharge (CCDC).

2.2.1 CV: Cycling Voltammetry

In the CV, a triangular voltage is applied in a cyclic manner. It varies from a minimum to a maximum with a settable slope called scan rate, measured in mV/s [3]. Then the current is measured and is reported in function of the applied voltage. Because the current flowing through a capacitor can be seen as in the equation 2.1:

$$I = C \cdot \frac{\Delta V}{\Delta t} \quad (2.1)$$

where 'C' is the capacitance, 'V' the voltage applied and 't' the time, for an ideal capacitor, the current in this technique should be constant positive, when the voltage rises, and constant negative, when the voltage drops. However, thanks to some resistance effect, this can rise or drop following the voltage behaviour as shown in the figure 2.4.

How is possible see in the figure 2.4, some time the current has some peaks. These are referred to chemical reactions: depending by the type of capacitors, these peaks could be wanted, as in the pseudo-capacitance, or unwanted like in the EDLCs. This technique is used to evaluate the capacitance of the device simply inverting the equation 2.1 [3].

Because the measure gives also information about the charge, is possible calculate the Coulombic Efficiency η , defined in the equation 2.2:

$$\eta = \frac{Q_D}{Q_C} \quad (2.2)$$

where ' Q_C ' is the charge when the device is charging, instead the ' Q_D ' is the charge when the device is discharging [15]. More this value is near to one, more the SC works correctly, because means that the loss of charge is low.

In theory, the Coulombic efficiency should be constant until a certain voltage, above which begins to decrease: this voltage is exactly the maximum voltage window that can be applied and must be found for the balancing of the areas.

To set a CV measure is necessary set different parameters. The CV presented in this thesis, are tested first with different voltage values to find the maximum voltage window and then, in a fixed voltage to see the variation in the time. The scan rate

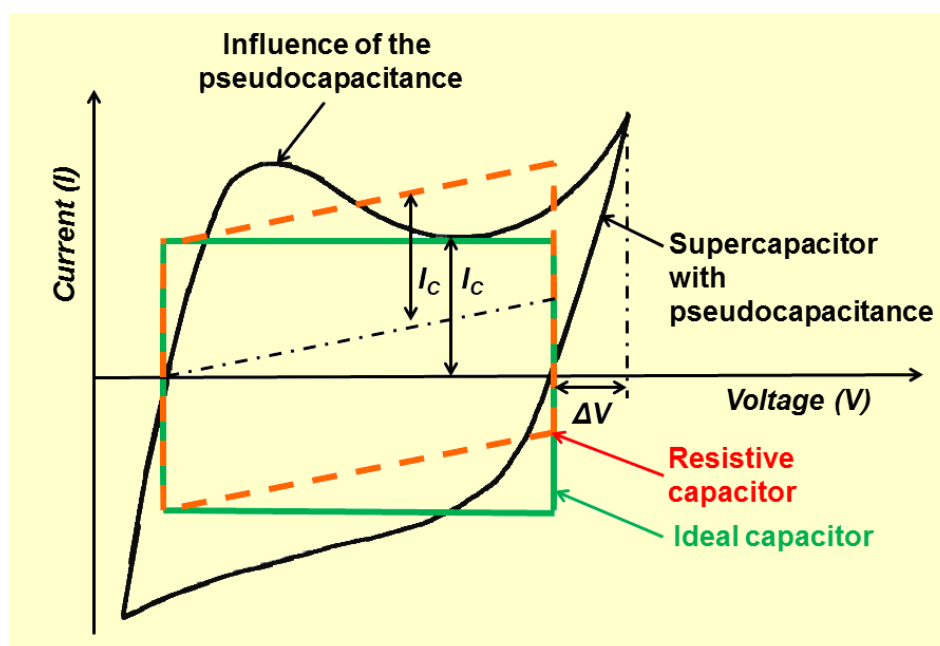


Figure 2.4: Comparisons between different CV of different devices. On the vertical axis is present the current, instead on the horizontal axis there is the voltage applied. In green, is possible see the behaviour of an ideal capacitor. In red, the behaviour of a capacitor with a resistive component and in black the behaviour of a pseudo SC. On the left of this latter curve is present a peak typical of a reaction present in the pseudo-capacitor.

used is of 1 mV/s, 2mV/s and 5 mV/s. Typically, more is slow the scan rate, more is done time to create possible reactions between electrode and electrolyte. So, a slow scan rate of 1 mV/s or 2mV/s is chosen to be sure of the absence of reactions. An higher scan rate of 5 mV/s, instead, it might be useful to setup more scans for specific windows, to make sure that efficiency does not decrease over time. Finally, also the number of scans must be set. This may vary, but in this thesis it will be varied from 10 to 50. An high number of scans is preferable to be sure that the efficiency stabilizes and does not degrade. However, if a small number, such as 10, is required for stabilisation, it may be useful to set a low number of scans to decrease the measurement time.

2.2.2 EIS: Electrical Impedance Spectroscopy

The aim of this technique is evaluate the impedance of the device at different frequency's values. To do this, is applied an alternate input voltage and for each setttable frequency of this is measured the current. Knowing the both, is possible

obtain the impedance. The results are typically shown in three plots: Nyquist, Lissajous and Bode.

The first represents on the y-axis, the imaginary part of the impedance, instead on the x-axis, is present the real part, evaluated for different frequencies.

The Lissajous shows the relation between the applied voltage, on the x axis, with respect to the measured current, on the y axis. Because the applied voltage and so the measured current, has a finite amplitude, the resulting figure is a closed shape, like an oval.

The Bode plot instead shows the magnitude and the phase of the impedance with respect to the different applied frequency.

These graphical representations are useful to understand the electrical model present behind the SC, but also to have an idea of the value of capacitance and of resistive component.

Looking at the figure 2.2 is possible see that the SC simply is a device in which is present a capacitive and a resistive effect. The capacitance is due to the electrical double layer or the pseudo-capacitance, depending by the type of SC. About the resistance instead is possible define two contributions: the ESR, Equivalent Series Resistance, and the IR, the Internal Resistance. Taking as reference the figure 2.2 is possible define the ESR as in the equation 2.3 and the IR as in the equation 2.4:

$$ESR = \lim_{f \rightarrow \infty} Re\{Z(f)\} \quad (2.3)$$

$$IR = \lim_{f \rightarrow 0} Re\{Z(f)\} \quad (2.4)$$

where 'Z' is the overall impedance seen between the two electrodes. From this equations is possible describe the ESR as all the resistive components that are in series with the capacitance, so the contacts and the electrolyte resistance. Typically the latter is the predominant contribution because the contacts could be neglected. The IR instead is an overall value that take in consideration all the possible resistances present in the SCs. Both could be found thanks to the Nyquist plot where is possible find the real part of the impedance at high, "infinite", and low, "zero", frequency value. As said before, thanks to the shape of the Nyquist plot is possible derive the equivalent electric circuit correspondingly of the SC. One first consideration is split the two families of the SCs: the EDLC and the pseudo-capacitance.

Starting with the EDLC, in the figure 2.5 on the left, is shown a representation of the device simply considering a capacitance in series with a ESR, while on the right is shown the correspondingly Nyquist plot.

However looking at the figure 2.2 is possible see that the figure 2.5 is not a valid simplification, because the two impedance parallel to the capacitors are omitted. In the EDLC, the impedance parallel to the capacitance (figure 2.1) could be seen

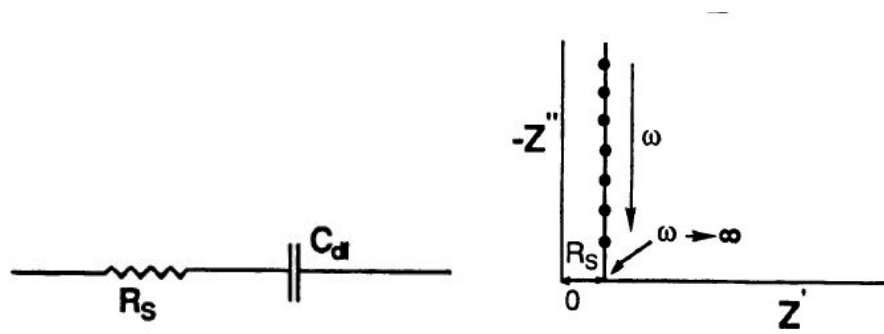


Figure 2.5: On the left simply representation of an EDLC consisting by the series of the resistance ESR, ' R_s ', and the capacitance of the EDL, ' C_d '. On the right the correspondingly Nyquist plot [5].

as a resistance. In this kind of devices, the faradaic reactions are unwanted so the value of this resistance must be very high, ideally infinite. For this reason, they could be omitted. If instead is necessary a more precise analysis they could be considered: the Nyquist plot of a resistance in parallel to a capacitance is a semi-circle with a diameter equal to the parallel resistance, so high. If are analysed only a range of frequency, like from 10 mHz to 1 MHz, is seen that they live in the place of the semi-circle in which the semi-circle could be seen as a line, justifying the model used in the figure 2.5.

The EDLCs that will be tested in the following sections, consist of porous materials. These pores create a diffusive process that changes the circuit, creating as figure of merit the image 2.6.

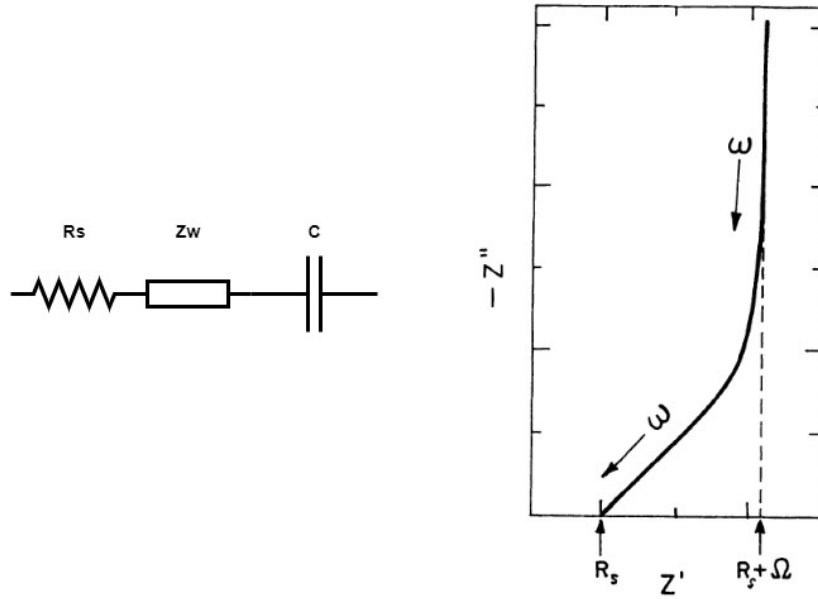


Figure 2.6: On the left simply representation of an EDLC consisting by the series of the resistance ESR, ' R_s ', the capacitance of the EDL, ' C ' with the adding of a diffusive element ' Z_W '. On the right the correspondingly Nyquist plot where ' Ω ' represents the electrolyte resistance within the pores [5].

For the psuedo-capacitor instead the circuit model with the correspondent Nyquist plot is shown on figure 2.7.

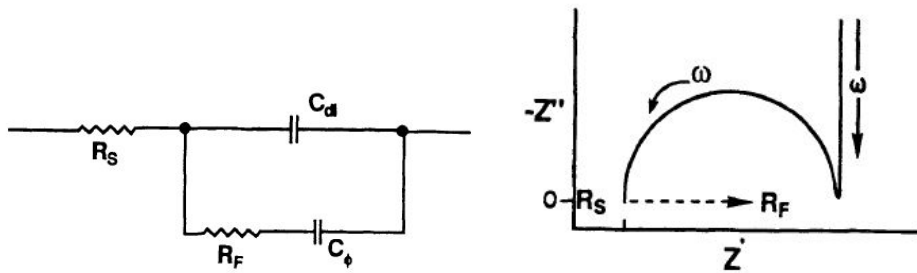


Figure 2.7: On the left, complete representation of an pseudo-capacitance consisting by a resistance ' R_s ', contact and internal resistance, a capacitance ' C_{dl} ' of the EDL, in parallel to the faradaic impedance. The latter consists of a faradaic resistance ' R_F ' in series to the faradaic capacitance ' C_ϕ '. On the right the correspondingly Nyquist plot [5].

Also in this case the curve can be more horizontal due to diffusive phenomena.

In this case, this can be caused by an excessive thickness of manganese dioxide as it will be shown in the next sections.

This Nyquist plot is used with the Bode plot to have a visual check of the correct behaviour of the SC. Furthermore is used to derive the ESR of the device that, in some cases, can be evaluated also at the frequency is 1 kHz [3].

Finally with the EIS is possible derive the capacitance to have a further check with the value obtained with the CV. Because the impedance of the capacitor ' Z_C ' can be evaluated as in the equation 2.5:

$$Z_C = \frac{1}{j\omega C} \quad (2.5)$$

where $\omega = 2\pi f$ with 'f' is the frequency, inverting the equation is possible obtain 'C' as in the equation 2.6:

$$C = -\frac{1}{2\pi f \text{Im}(Z_C)} \quad (2.6)$$

where 'f' is the lowest frequency applied and ' $\text{Im}(Z_C)$ ' is the imaginary part of the impedance at that frequency [3]. Another possibility is calculate the capacitance as expressed into the equation 2.7:

$$\text{Re}\{C\} = \frac{-\text{Im}\{Z_C\}}{\omega |Z_C|^2} \quad (2.7)$$

where $Z_C = \sqrt{\text{Re}\{Z_C\}^2 + \text{Im}\{Z_C\}^2}$ is the complex impedance [16].

For the measures, like for the CV, also the EIS has some parameters that must be set. In the following EIS the frequency is varied from 10 mHz to 1 MHz instead the signal sent is sinusoidal with an amplitude of 5 mV of peak.

2.2.3 CCDC: Constant Current Charge and Discharge

The CCDC is a technique similar to the CV, but in this case is set a constant current and is measured a voltage. The current is set as a constant positive, charge phase, and negative, discharge phase, and between the two could be present a dwelling period in which the voltage remains constant. For a ideal capacitor the resulting voltage into the time should be a perfect triangular shape. As already said, the EDLC is not an ideal capacitor, but there is also a resistive component. For this the result shape of the voltage into the time is shown in the figure 2.8.

Thanks this technique is possible evaluated the ESR and the capacitance. Looking at the figure 2.8 is possible see a drop into the voltage due to the ESR. In fact is possible evaluate the ESR as in the equation 2.8:

$$ESR = \frac{\Delta V}{\Delta I} \quad (2.8)$$

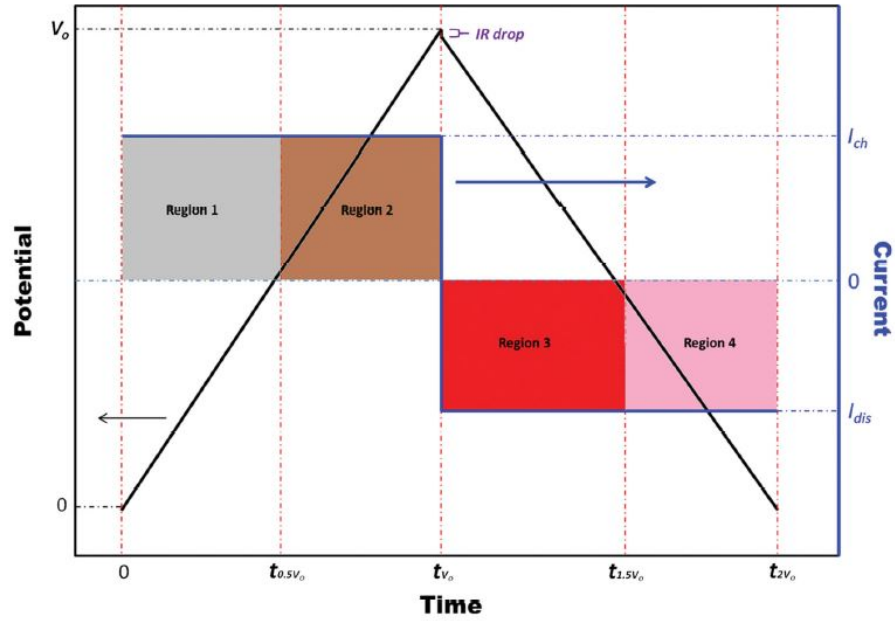


Figure 2.8: CCDC result. On the left y-axis, the voltage recorded over time is present, on the right y-axis the applied current over time. The voltage presents a drop in the peak called IR drop [3].

where ' ΔV ' is the IR drop of the voltage and ' ΔI ' the charge or discharge current. The capacitance is instead evaluated as the in the equation 2.9:

$$C = \frac{I_{dis} \Delta t_{V_0-2V_0}}{V_0 - V_{IR-drop}} \quad (2.9)$$

where ' I_{dis} ' is the discharge current, ' $\Delta t_{V_0-2V_0}$ ' is the discharge time and ' $V_0 - V_{IR-drop}$ ' is the variation of the voltage without the IR drop.

For all the measures that will be shown in the following sections, the device is always first analysed with an EIS to be sure that the device properly works and is properly closed. From this is derived the ESR and an approximate value of the capacitance. Then, the CV is used to characterize the materials finding the maximum potential window and the correspondingly value of capacitance. Finally the CCDC is used to see the variation of the performance during the time.

2.3 Electrolyte

The electrolyte plays a very important role in the SCs. It impacts the performance of the device, the cost, the environmental and the safety.

Have a good performance means, as already said, high potential window but means also high ionic conductivity and high stability.

The conductivity in fact impacts on the resistance of the electrolyte: more is high, more the ESR is low. Instead the stability can permit the use over the time.

The state of the art is trying to exploit new types of electrolyte that can have all these features, but nowadays is still necessary a trade off .

The aqueous electrolytes present an high conductivity so low ESR, low cost of production and are environmentally friendly. These are divided into acid, neutral and basic [9] .

The neutral electrolytes present a lower ionic conductivity with respect to the other and so an higher ESR, but having less $[H]^+$ and $[OH]^+$ that acid and basic's electrolytes should have an higher potential window "postponing" the oxygen and hydrogen evolution. For this reason it has been chosen to use as electrolyte the neutral Na_2SO_4 in a concentration of 1 M. Because is neutral, the pH of the Na_2SO_4 is constant to 7.

This information about the pH could be important to have an idea of the potential window of the device. In fact the Pourbaix's diagram, is a graph that shows the stability conditions of a material under different pH of aqueous solution.

As said the SC has a substrate of gold. Considering the Pourbaix's diagram shown in the figure 2.9 of the gold, is possible have an idea of the maximum cathodic and anodic potential windows if the device consists only by gold.

From this figure is possible see that the maximum applied potential is of 1.2 V, that is the typical potential of an aqueous electrolyte. Above, the electrolysis process of the water begins to appear. Increasing the pH is also possible notice that there is a shift of the window from the anodic to the cathodic. If the neutral electrolyte is changed with a basic, like the very used KOH, what is expected is a shift of the window towards the cathodic voltages, as demonstrated by the figure 2.10.

The electrolyte doesn't contain the chlorine and so is necessary understand if the created reference wire of Ag|AgCl works well in this; if it is not, is necessary change the reference. One first idea to be sure to overcome the problem is maintain the reference in HCl and then put this in the aqueous solution. However it is not realizable, because, when the current collector is put into an open cell fill with an high quantity of electrolyte to assure the presence also of the reference, there is a delamination process of the electrode, that completely destroys it. So another possibility is create a salt bridge between the two electrolytes, but with this set-up the reference is far by the electrode, the resistance is high, is unknown the voltage

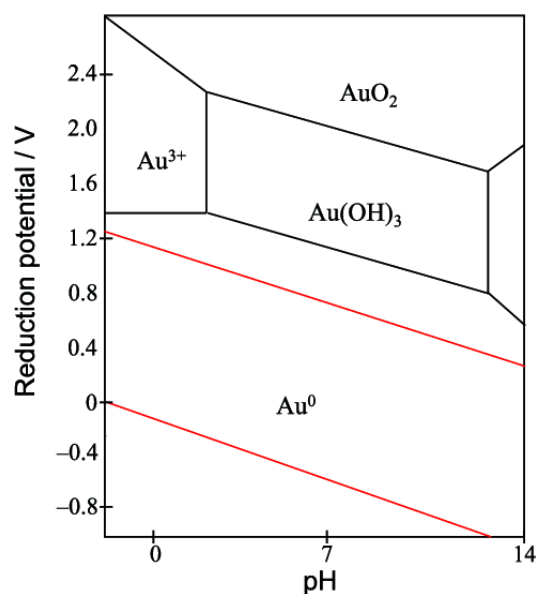


Figure 2.9: Pourbaix's diagram of the gold. On the y-axis are present the reduction potentials. On the x-axis is present the pH of the electrolyte solution. In the plot are present different zones: in each zone is written the type of material that is created under that voltage and pH solution [17].

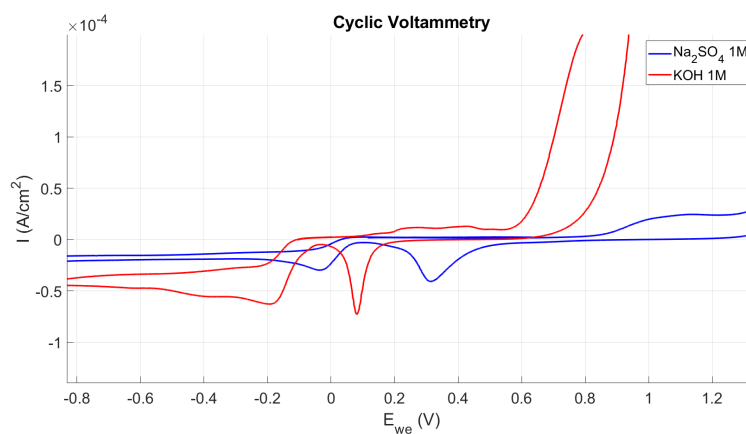


Figure 2.10: CV comparison between bulk gold in Na_2SO_4 1M and KOH 1M. The CV is set into a open cell with 50 ml of solution and using as reference the $\text{Ag}|\text{AgCl}$ 3M in KCl of the Metrohm. The counter electrode is a platinum wire and the scan rate is set at 1mV/s. How it is possible see, the two CV are very similar, only shifted due to the different pH of the electrolyte.

drop between this and so is lost the idea of the reference.

The only possibility is test if this reference can work also in other electrolyte, maybe having a small variation on the open circuit potential, but limited during the time of the measurement [14].

For this reason is created an open cell with:

- Working electrode: Ag|AgCl wire created as described in the previous section. This is dipped in 1M Na_2SO_4 solution because the aim is understand if it changes its potential over the time.
- Reference electrode : Ag|AgCl in 3 M KCl of the Metrohm company. It sure works as reference because the Ag|AgCl wire is dipped in a solution in which is present the chloride. Then the reference and its electrolyte are put into the 1M Na_2SO_4 solution. Is possible a contamination between the two, but is very small for the time of the experiment and so it could be neglected.
- Counter electrode: platinum wire.

Then the OCP is measured for 24 h and the result is shown in the figure 2.11.

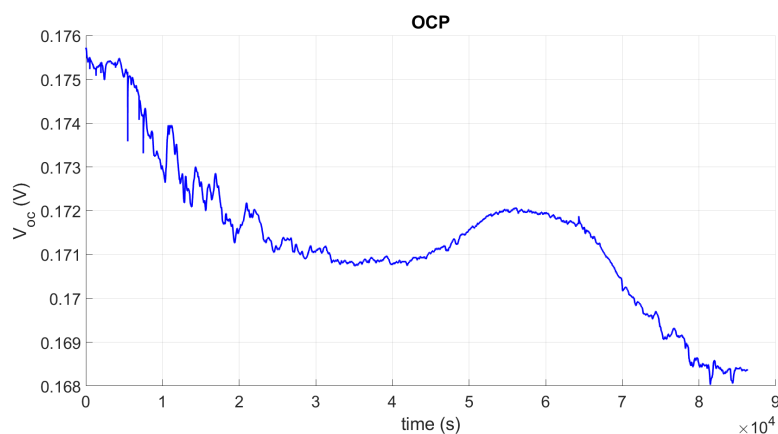


Figure 2.11: Potential measurement of the Ag|AgCl wire in 1M Na_2SO_4 refereed by the Ag|AgCl of the Metrohm company in 3M of KCl. This potential is monitored for 24 hours that are 86400 s.

The idea is measure for 24 h because the following experiments have a duration less of this, so if there is not a significant variation of the voltage in this time, means that there is not a variation also doing other smaller measures. From this result is possible see that the variation is from 0.176 mV to 0.168 mV so in 24 hours there is a change in the potential minus that 10 mV. This very small variance is acceptable and so this could be used as reference electrode also in this aqueous electrolyte. In this case it is called 'pseudo-reference'.

2.4 Current collector

2.4.1 Substrate

The substrate is the starting point of the electrode. Thanks to different techniques, it is possible to deposit the active materials on it creating the μ SC.

The most used substrate in the electronic application is the silicon. It is a semiconductor material that can be doped varying its propriety and that can be used for lithographic process. On the other hand, the silicon has rigid substrate and if are looked application like wearable devices this can become a problem. For this reason it is necessary to study a flexible substrate like the flexible polyimide Kapton. To put the active materials on it, it is first necessary to deposit the adhesion layers that make the deposition possible. The material chosen to enter in contact with the active materials, is the gold that does not attack to the substrate: for this is placed a titanium layer between the gold and the Kapton [18]. These are deposited thanks to a physical vapour deposition: evaporation. A layer of 10 cm x 10 cm of kapton is put into the chamber. The chamber is then brought to a pressure of 10^{-9} bar. Taking 30 mg of titanium, putting it into a crucible and sending a current of 180 A it is possible to deposit 20 nm of Ti.

Without opening the chamber, so with the same conditions, another crucible is filled with 300 mg of gold and applying a current of 160 A it is possible to deposit 150 nm of gold.

This information about the thickness of the layers are experimentally obtained thanks to a quartz oscillator put into the vacuum chamber. To be sure of the result also a sheet resistance measured is done and this confirmed the result.

2.4.2 Electroplating of the gold

The state of the art about the SCs moves towards an increase of the energy density. The equation 1.2 shows that this result could be reached increasing the capacitance and so, looking at the equation 1.1, increasing the superficial area.

For this reason, above the planar gold layer is so grown a 3D gold layer with an electroplating process. This is not done for both the electrodes, but only for the electrode that will be covered with carbon-based materials. In fact, the carbon particles can link more easily with the porosity of the gold with respect to a planar layer. On the other hand, the planar gold is useful for the deposition of manganese dioxide.

The electroplating process is a metal deposition technique in which are present two electrodes immersed in a solution. One is the sacrificial anode layer of gold, whose aim is "loss" the gold's ions to deposit and the other is the cathode layer where is wanted to do the deposition. Applying a current between the two, the

first losses ions into the solution, that works as bus, while the second reaches these ions, where are deposited. Because the gold ions into the solution are positive, is applied a negative current at the working electrode. The solution used for the transport of the ions is the commercial solution "NB semiplate 100" that is properly for deposition of gold. This means that in reality a sacrificial layer of gold is not necessary because the gold ions are already present in the solution: however a gold sacrificial layer of gold is put to maintain unchanged the gold's ions concentration in the solution over the time.

The commercial solution was born with the aim of grow a planar layer of gold on bulk material, but the aim in this case is grow a dendritic layer with an high superficial area on thin layer. For this reason is necessary find a set of parameters different by the set parameters suggested by the industry.

The electrode consists of thin layers so the deposition is more complex than a bulk electrode. The idea is so start with the test on the bulk layer just to see if it is possible the deposition and then move towards thin layers, maybe changing the parameters.

This choice is done both to save cost for the samples and to save time: if is impossible with a bulk material, is very difficult that it could be possible with thin layers.

So to do this, sheets of 50 μm of titanium are taken and cleaned in a sonicator in which there is a solution with :

- 1/3 % v/v of ethanol,
- 1/3 % v/v of acetone,
- 1/3 % v/v of distilled water,

for 30 minutes.

Then the electrodes are completely dried in a dryer for all the night. Because on the surface is possible the formation of a titanium oxide, before the plating, the electrodes are put in a solution contain :

- 1/3 % v/v of ammonia hydroxide,
- 1/3 % v/v of H_2O_2 ,
- 1/3 % v/v of distilled water,

for 30 seconds to remove this possible oxide formation.

For the electroplating the set-up is the following:

- the electrode works as cathode (-),
- the sacrificial layer works as anode (+),

- the distance between the two electrodes is of 3 cm,
- the current density is varying from 0.5 mA/cm^2 to 2.5 mA/cm^2 with a step of 0.1 mA/cm^2 ,
- time of 10 minutes,
- the temperature is the room temperature of $20 - 25^\circ \text{ C}$.

The results are shown in the figure 2.12. Increasing the number of the samples, the current density increases with a step of $+0.1 \text{ mA/cm}^2$. It is possible to see that the electrodes obtained with small current density have a thin layer of gold deposited above, seems practically zero, but the visible yellow gold increases with the increasing of the current. This is true until the sample number '13': passing from 1.6 mA/cm^2 , sample '12', to 1.7 mA/cm^2 , sample '13', it is possible to see a visible difference of the different deposited gold. Above this, there are not visible differences.

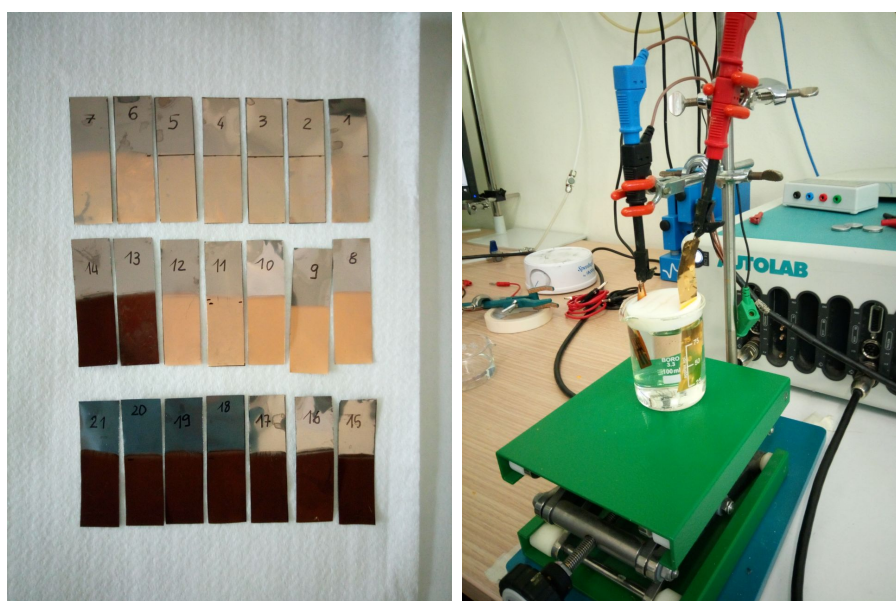


Figure 2.12: Electroplating deposition. On the left, electrodes of $50 \mu\text{m}$ of titanium after a gold electro-plating. The electrode number '1' is fabricated with a current density of 0.5 mA/cm^2 , the number '2' with 0.6 mA/cm^2 and so on, until the number '21' fabricated by a current density of 2.5 mA/cm^2 . The other parameters like temperature, distance and time are fixed. On the right, a photo of the set-up where it is possible to see the sacrificial layer on the right and the sample on the left.

Measuring the mass before and after the electroplating and dividing by the area, is possible obtain a calibration curve shown in the figure 2.13. From this curve

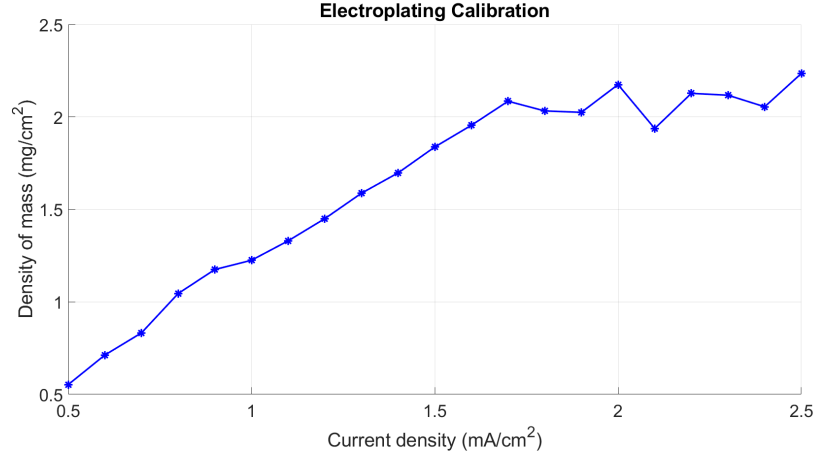


Figure 2.13: Calibration curve for bulk electroplating process. On the y-axis is present the density of mass deposited with a specific current density indicated on the x-axis. The points from the left to the right are correspondingly to the electrode '1', '2', '3'...'21' shown in the figure 2.12.

is possible see that increasing the current density, the deposited mass on unit of area increases. This is true until the sample '13' above which the mass seems to be stable. This result is coherent with the visual result shown in the figure 2.12, in fact at the beginning the quantity of yellow increases and then all the samples seem to be equals.

Because the aim is deposit a 3D gold layer, this means that is necessary a current density above 1.7 mA/cm^2 with a distance of 3 cm, but seems, from this result, that increasing the current, the deposited mass remains constant.

To limit the cost, this calibration curve is done only for one sample to each current density step. This means that there could be variations on the deposited mass applying the same conditions, but the aim is just to have an idea at what happens increasing the current density and if is possible deposited amorphous, 3D, gold.

Now is necessary repeat the experiment with thin layers instead that bulk layer. Using the same parameters the device begins to delaminate. For this reason the distance has increased of 1 cm, from 3 cm to 4 cm, and the time has decreased, from 10 minutes to 7 minutes choosing to use from the previous result a minimal current density of 1.7 mA/cm^2 . This time the result is reached, however from the previous measure, is possible see that above a certain current threshold, the mass deposited is unchanged: increasing this, means only increase risk of stress. For this reason the current density has decreased at 1.5 mA/cm^2 , under which the dendritic

deposition disappears.

So the parameters used for the electroplating deposition of gold on a seed thin layer are:

- time : 7 minutes,
- current density: 1.5 mA/cm^2 (the '+' is on the sacrificial layer),
- distance : 4 cm.

Measuring the voltage during the deposition is possible obtain the figure 2.14. What

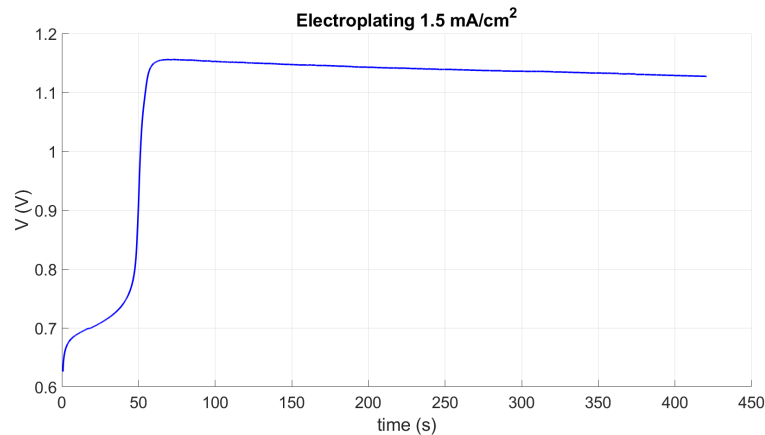


Figure 2.14: Voltage recorded during the electroplating deposition of gold at 1.5 mA/cm^2 . How it is possible see the voltage stabilises at 0.7 V for a small time and then increases up to 1.15V. Exactly after this point, the deposition passes from planar to dendritic.

is important to notice from this curve, is an "activation" of the process after 50 s. During this time the deposition is planar instead after begins to be dendritic. If the current is not sufficiency high, so lower than 1.5 mA/cm^2 , what is experimentally seen is a stabilisation of the potential at about +0.7 V or less for all the time and the absence of dendritic structures on the electrode.

Of course maybe these are not the only possible parameters to do a plating process. These are parameters for which the process correctly works and is repeatable and for this are chosen.

With this settable parameters is possible deposit 1.5 mg/cm^2 , with a variance of 12 % mainly due to the different layouts of the layer on which the deposition is done. The deposited layer has a dendritic shape on some μm as shown in the image 2.15.

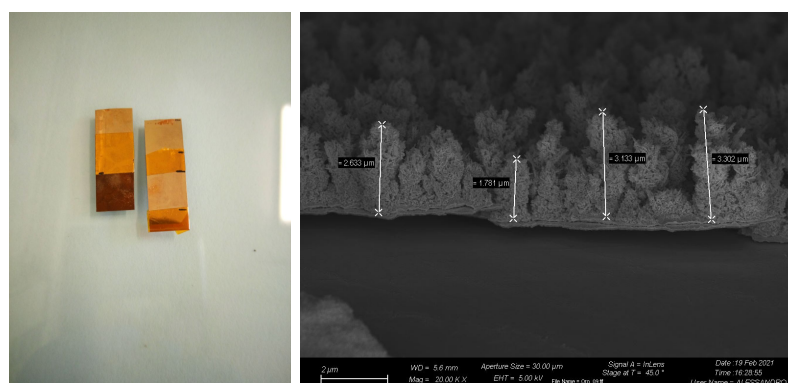


Figure 2.15: 3D gold deposition. On the left a visual comparison between planar (yellow) and 3D gold (brown). On the right a Fesem image of dendritic gold deposition. The dendrites have an height of some micrometers and is possible see the porosity and the increase of the area that they introduce.

2.4.3 Characterization of the current collector material

Once that the current collector is created, is necessary test it to understand its propriety. These test are done because if the active materials will not perfectly cover the electrode, is important understand what happens when the current collector enters in contact with the electrolyte.

To do this, is need choice a cell, a closer and set the parameters for the measurement. To be sure that the gold and the 3D gold don't create reactions with the electrolyte, they are simply test in a open cell. 50 ml of 1M Na_2SO_4 is put into a Becker in which are immersed the working electrode with kapton, titanium and gold, the reference electrode of the "Metrohm" company in 3M of KCl and a platinum counter electrode. The result is a complete delamination of the sample.

To by-pass this problem, a bulk gold layer is tested in the same conditions. To avoid some contamination the electrode is before cleaned with a polishing technique done first with a diamond (abrasive particles of 1 μm) polishing and then with an alumina (abrasive particles of 0.3 μm) polishing. The EIS graphs of results are shown in the figure 2.16.

What is important notice is the behavior obtained with the CV shows in the figure 2.17.

How it is possible see there are not reactions in the cathodic potential window, but there are also peaks in the anodic, maybe due to the oxidation and then to the reduction of the gold. The two peaks at the extremes are done instead by the oxygen and hydrogen evolution.

Because the superficial layer can be composed of dendritic gold and not only by planar gold, this test is repeated with a plating of 3D gold, producing similar

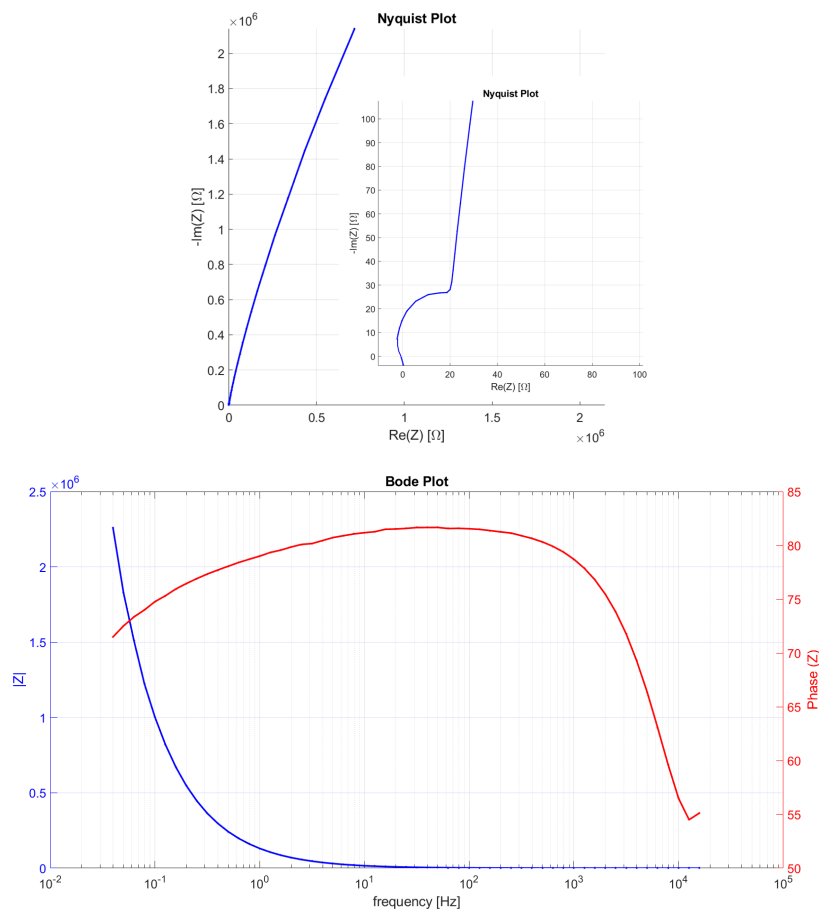


Figure 2.16: EIS of a bulk electrode of gold in 1M Na_2SO_4 . Above there is the Nyquist plot: the ESR is low, but being an open cell it depends by the distance between the reference and the sample. Under there is the Bode plot: the phase is about 80° and decreases a bit at low frequency.

results being the same material.

Now is necessary test the thin layers putting a small amount of electrolyte to avoid the delamination. To do this it is necessary to change the cell configuration from an open cell to a pouch cell. To characterize the electrode is used a stack configuration in which on the 3D gold is put the reference and the counter electrode, separated by the fiber glass filled with $500 \mu l$ of solution. The overall cell is closed in a pouch to prevent evaporation of the electrolyte and to apply a pressure so that the electrodes are close together. This time the electrode is not only made of gold, but there is also an under layer of titanium. Furthermore the reference is near to this, so that the chlorine that can go into the solution can reach the surface of the electrode.

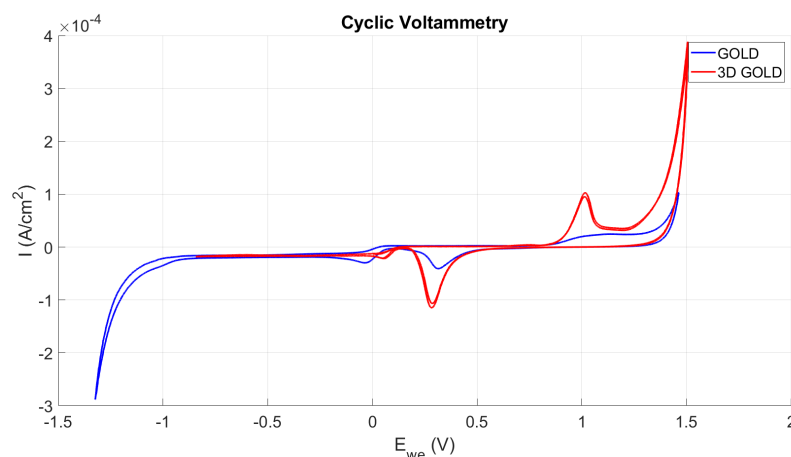


Figure 2.17: CV of a bulk electrode of gold in 1M Na_2SO_4 , blue line. The window is from -1.4 V to +1.5 V. To do a comparison is shown also the CV of a bulk electrode of which are grown 3D structures, in red. The reactions are the same, but the magnitude of the 3D is bigger.

Because this can react with the titanium, this can create problems. To be sure of this hypotheses, the bulk electrode used for the calibration curve is tested, to see if this titanium layer can create problems. It is chosen to use this electrode to limit the cost and because the aim of this measure is just see if the titanium can react, also covered by gold. It is tested in a proper electrochemical cell "EL_CELL" for aqueous electrolyte doing a three electrodes measurement because this electrode has a conductive substrate. This cell could be an optimal solution to all the tested electrodes, however these can not be used with the kapton because it has not a conductive substrate.

The cell consists of:

- Working electrode : sheet of 50 μm of titanium on which is deposited 3D gold. The parameters of the electroplating are 3 cm of distance, current density of 2 mA/cm^2 and a time of 10 minutes.
- Separator: glass fiber of 675 μm filled by 500 μl of 1M Na_2SO_4 .
- Reference electrode : wire of Ag|AgCl. This is put exactly in the middle of the fiber glass so it is in a distance minor of 400 μm by the working electrode.
- Counter electrode: disk of carbon materials.
- Spacer to increase the pressure of the cell.

The first characterization measure done is an EIS which graphs results are shown in the figure 2.18. This measurement is done from a frequency of 100 kHz to a

frequency of 10 mHz.

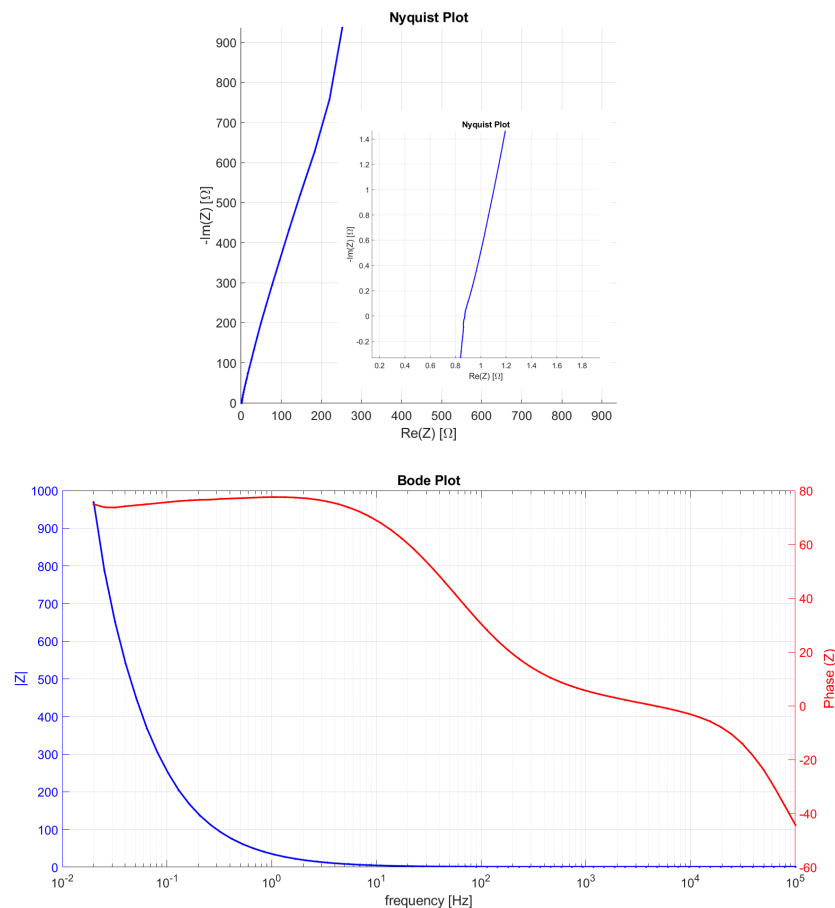


Figure 2.18: EIS of a bulk electrode of titanium on which is plating the dendritic gold. Above there is the Nyquist plot, on the left a full scale view, on the right a zoom: the slope is good and the ESR is of 0.82Ω . Under there is the Bode plot: the phase is about 80° and remains constant also for low frequency.

These EIS results are similar to the theoretical results shown in the figure 2.7, having also a very small series resistance of 0.82Ω .

For this reason also a CV measure for the anodic and cathodic windows is done and the results are shown in the figure 2.19. This figure shows superimposition of different CV done increasing the potential window with a scan rate of 2 mV/s on the left axis and the correspondingly Coulombic Efficiency on the right axis.

For each window the CV is repeated 10 times: this small number of cycles is, in this case, sufficiency to stabilize Coulombic Efficiency that is about constant on

the different voltage for the anodic at 86 % with a density of capacitance of 8 mF/cm^2 , instead for the cathodic the Coulombic Efficiency is not constant and the density of capacitance is 2 mF/cm^2 . To evaluate the density of capacitance is used the substrate area. Of course the real area with the dendrites is higher, but is impossible evaluate how much is higher. So, from this point, all the time that is shown a density of capacitance for unit "area", the area is the substrate area.

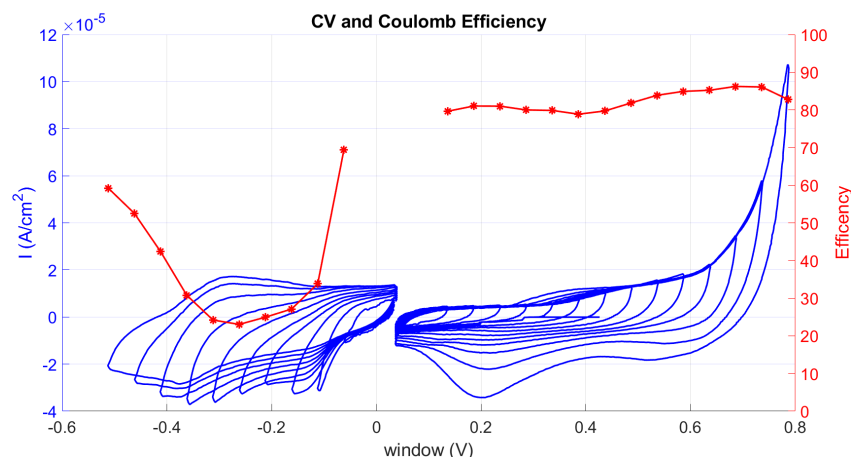


Figure 2.19: CV and Coulombic Efficiency of a bulk electrode of titanium on which is plating the 3D gold. Superposition of the anodic potential windows and the cathodic potential windows.

What is important understand from this CV, is the shape. In fact, in the cathodic window, is possible see the reaction peaks. These peaks appear in the expected range for the reactions of the titanium and so the hypothesis is confirmed. Although these reactions are reversible because very near, is possible change the adhesion layer of the electrode from the titanium to the chromium. This choice is done because both the adhesion layers work well and can be deposited easy with the same procedure, but the chromium doesn't react in these potentials. The only difference is a change into the set-up parameters for the evaporation deposition, putting 30 mg of chromium with a current of 180 A instead of the titanium.

The final current collector used for the creation of the electrode is so done by 20 nm of chromium and 150 nm of planar gold.

Repeating the characterization is shown that the gold above a chromium layer, doesn't create reactions in the cathodic windows. For the anodic, it oxidises and reduces but at high potential, over the field of potential under study. So the aim of the following measures is compare the difference between the gold and the 3D gold

and collect data useful to further comparison, once that active materials will be deposited, justifying why will be deposited.

The current collector is tested in the same pouch cell described above, and from this point, it will always use this closer.

Above the electrode under test is put the reference wire of Ag|AgCl and the counter-electrode separated by 675 μm of fiber glass, filled by 500 μl of Na_2SO_4 . The cell is so closed in a pouch cell. To create the contacts there are different possibility. For availability and cost is decided to use titanium's grid. Of course, this will react as described above. However, as said, these reactions are reversible so don't create problems and this time the material is not inside the device but works only as contact. If is wanted a characterization without these reactions, is simply possible change the contact material and not the substrate of the device.

The two tested current collectors are one with planar gold and the other with the dendritic 3D gold.

Remembering that the final device will consist of two different materials, the 3D gold will work as substrate for the carbon based materials.

As will be better explained in the following sections, the carbon-based materials' electrode will be work as cathode, instead the manganese dioxide as anode. For this reason, the current collector with 3D gold is tested only in the cathodic window, instead the planar gold in both.

The comparisons and the results of an EIS Nyquist measure are shown in the figure 2.20.

From this results is possible see the difference between the two, in particular the planar gold produces a capacitance of 0.06 mF/cm^2 with a ESR of 1.7 Ω while the 3D gold has a capacitance of 0.86 mF/cm^2 with a ESR of 2.7 Ω .

To do a correct comparison also a CV measure is done and the result is shown in the figure 2.21.

From this result is possible evaluate the change of capacitance summarized into the table 2.1.

In this case is possible see the reactions of the titanium that maybe can produce same errors during the evaluation of the capacitance, but if the current before the reaction peaks is evaluated, there is a difference of a factor of 3 between planar and 3D gold. In any case, is possible see a good increase of capacitance from the planar to the 3D gold.

The choice to use as maximum potential the -1V and a scan rate of 5 mV/s will be clear in the next sections, and these results are collected to do future comparison.

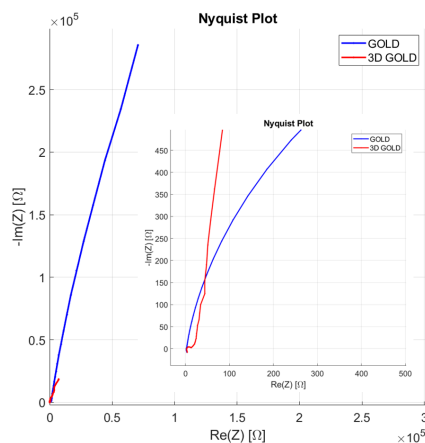


Figure 2.20: EIS Nyquist comparison of the planar gold, blue line, and the 3D gold, red line. On the left there is a full axis view, on the right a zoom. The range of frequency is from 1 MHz to 10 mHz.

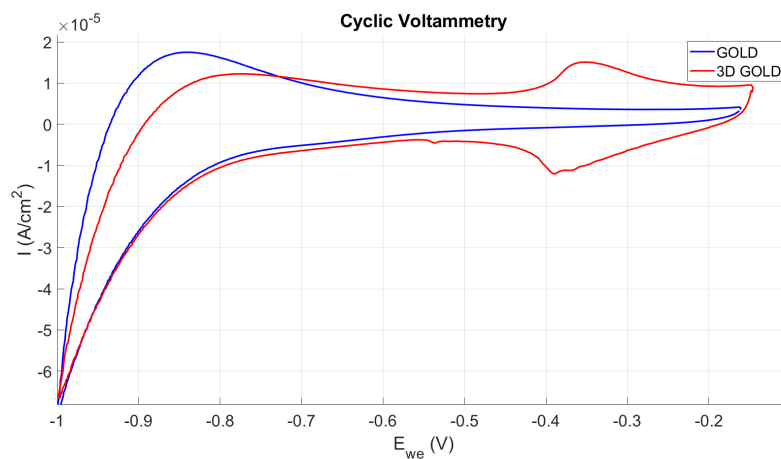


Figure 2.21: CV comparison between the planar gold, blue line, and 3D gold, red line. The scan rate is set at 5 mV/s and for each the number of scans is 30.

With regard to the behavior of the planar gold into the anodic window instead, the figure 2.22 represents a CV measure with a scan rate of 5mV/s until +0.7V for 30 cycles. Also in this case these parameters will be explained in the following sections. The capacitance is of $0.9 mF/cm^2$.

	C (mF/cm ²)	ESR (Ω)
GOLD	1.4	1.7
3D GOLD	1.7	2.7

Table 2.1: Comparison of the density of capacitance, 'C', evaluated with the CV and the equivalent series resistance 'ESR', evaluated with the EIS, of the two deposited gold types. The 3D gold have better parameters with respect to the planar gold. The sample has an area of 1 cm².

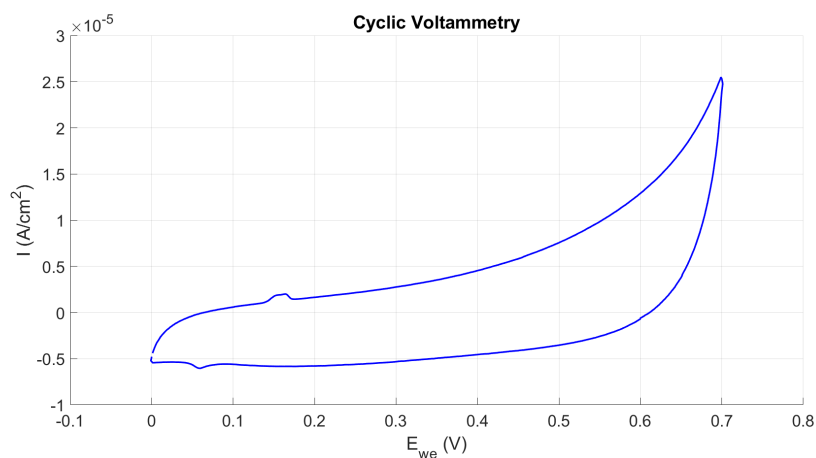


Figure 2.22: CV of planar gold, blue line, for the anodic window. The scan rate is 5 mV/s and for each CV the number of scans is 30.

Chapter 3

MnO₂ Electrode

The only current collector doesn't produce an high capacitance in the 1M of Na_2SO_4 and is not stable, for this reason is necessary to cover it with active materials. One possibility is covered it with manganese dioxide, using the pseudo-capacitance effect to create one electrode on the μSC .

To do this, there are different techniques as explained in the introduction section, but if the aim is create a planar device, the most convenient techniques are the techniques in which the deposition is due to the application of a current or voltage.

3.1 Electroplating deposition

The technique used for the deposition of the manganese dioxide is the same used for the 3D gold deposition. The only difference is the change of the set-up parameters.

3.1.1 Set-up

To do an electroplating deposition of manganese dioxide is taken as reference the [19].

On a polyimide film, is deposited by evaporation process an adhesion layer of chromium and a seed layer of gold. Directly on this layer, so without a plating of 3D gold, is deposited a manganese dioxide layer with an electroplating process.

The set-up cell is an open cell with a solution of 0.1 M manganese (II) acetate and 0.1 M of sodium sulfate in which is set a three electrodes measurement. As reference is used the Ag|AgCl 3M in KCl of the "Metrhom" company and as counter electrode a platinum wire. To set the current density and the time, also this time are done different trials to find the best parameters that produce a good result. It

is seen that a current density of -1 mA/cm^2 , with a distance of 2 cm, for 1 hour, produces good result avoiding the delamination of the samples. Also in this case, other set-up parameters can be used, but the those described above produce good and repeatable results. The recorded voltage is shown in the figure 3.1 where is possible see that the potential for the plating is constant at -1.4 V .

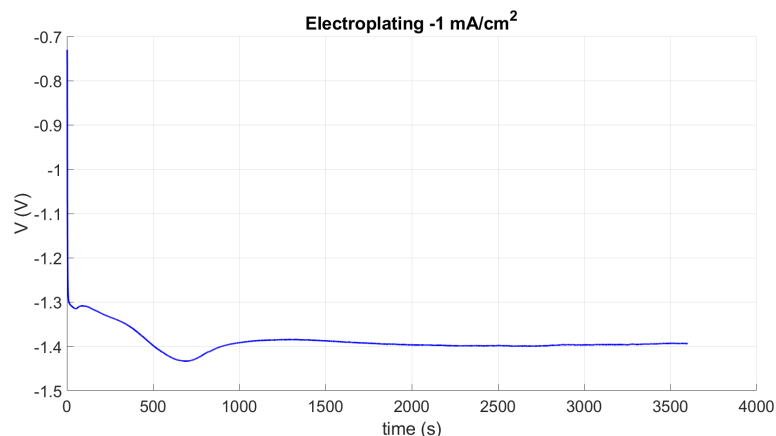


Figure 3.1: Voltage measured during the electroplating deposition. The current density is set at -1 mA/cm^2 where the working electrode ('+') is put on the sample. The area under test is of 1 cm^2 .

After, is carried out a calcination process as cited in the literature, but also this time the parameters are little bit changed to find the best for this type of substrate. For this, once that the electroplating is finished, the sample is dried at the room temperature for 2 hours. Then is put in the "Büchi" oven. The pressure in which is carried out the calcination process is the room pressure because is wanted the presence of oxygen in the atmosphere, to create the oxide. So the sample is brought for 1 hour at $60 \text{ }^\circ\text{C}$ for the complete evaporation of the solution on it, then at $300 \text{ }^\circ\text{C}$ for 4 hours, for the calcination, and finally another time to $60 \text{ }^\circ\text{C}$ to avoid an abrupt drop in temperature.

The electroplating is carried out with a three electrodes measure for the first times, to see the reaction potential shown in the figure 3.1. However, to save quantity of solution and avoid contamination of the reference electrode, with the consequence cleaning of this, the electrodes are after fabricated using a two electrodes measure in a set-up illustrate into the figure 3.2. In this figure on the left is also shown how as it appears the manganese dioxide before and after the calcination process. The images shown are of planar and interdigitated layouts because, as will be explained in the chapter '6', also these layouts are studied. In this case the aim of these images is just to see the difference about the deposited manganese dioxide. With this set-up is possible deposit 3 mg/cm^2 of manganese dioxide.

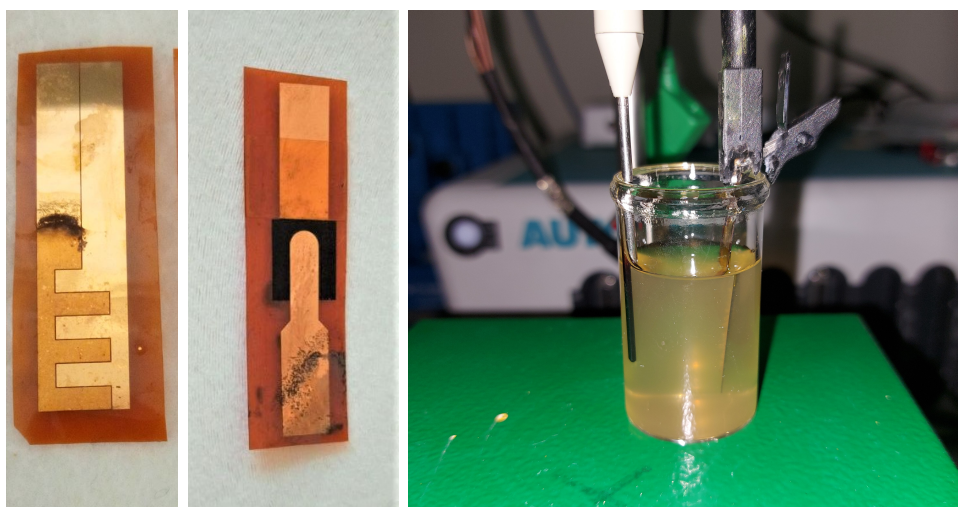


Figure 3.2: Manganese dioxide deposition. On the left the comparison between the planar gold with and without the manganese dioxide above. The first is before the calcination, the second after. On the right the two electrodes set-up for the electroplating deposition of manganese dioxide. In the latter, on the right there is the working electrode on which is applied a current density of -1 mA/cm^2 with respect to the counter electrode on the left. This set-up is only used to save quantity of electrolyte and is used only after the characterization at three electrodes.

3.1.2 Characterization

The manganese dioxide's electrode is before characterized with an EIS and then with a CV.

The EIS graphs results are shown in the figure 3.3.

From these results, is possible see the typical EIS due to a pseudo-capacitance contribution, as described into the previous chapter, with a ESR of 2.4Ω . So the test is followed by a CV.

For the CV test, the electrode is before tested on the total voltage window, from -0.9 V to $+0.9 \text{ V}$ just to have an idea at what happens at the cathodic and anodic windows. The result is shown in the figure 3.4.

How it is possible see from the figure 3.4, the manganese dioxide seems to work well into the anodic window, instead has limited current, so limited capacitance, into the cathodic window. For this reason, it is decided to use the manganese dioxide electrode only for the the anodic potential window. To find the maximum window that can be applied, a voltage from $+0.1\text{V}$ to $+1.3\text{V}$ with a step pf $+0.1\text{V}$ is studied with a CV for 20 scans at 5 mV/s . The CV result is shown in the figure 3.5. In this, is possible also see the correspondingly Coulombic efficiency of 97%

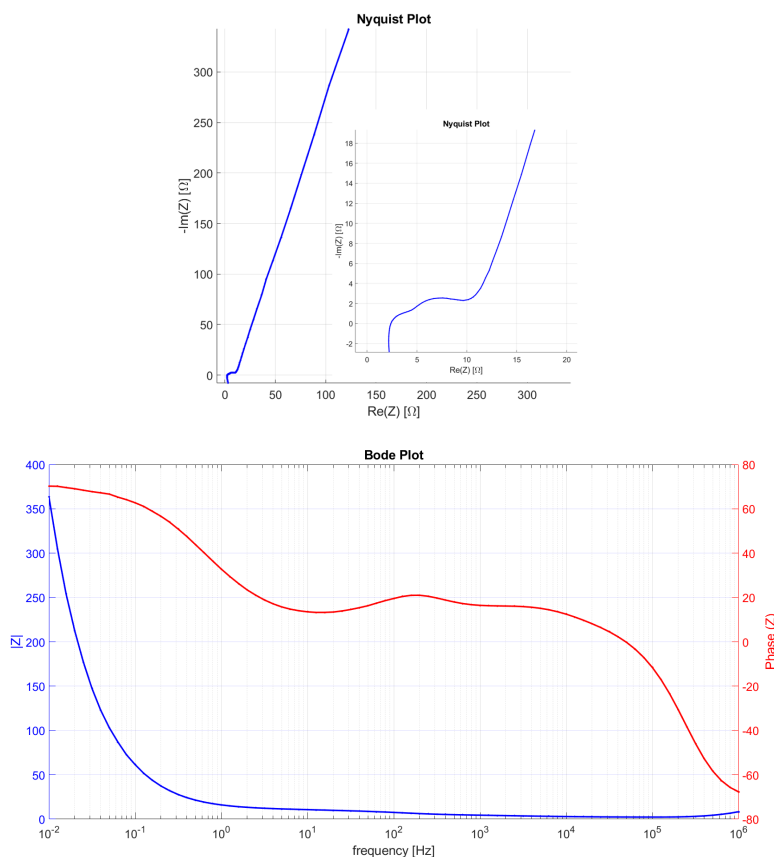


Figure 3.3: EIS graphs results. Above there is the Nyquist plot: the two images are the same, the left is with the full axis, the right is a zoom at high frequency. Above the correspondingly Bode plot.

until +0.7V, 95% until +1.1 V while, for higher voltage it begins to decrease.

If it is fixed as limit the first decreasing of the efficiency, the maximum anodic window is of + 0.7 V with a correspondingly density of capacitance of $62mF/cm^2$.

The substrate of the manganese dioxide consists of planar gold. The comparison between the gold with and without the manganese dioxide is shown in the figure 3.6. Considering from the previous characterization a capacitance density of $0.9mF/cm^2$, is possible evaluate that the adding of the MnO_2 produces an increase of the capacitance of about a factor 69, as shown also in the table 3.1.

The difference with respect to the planar gold and the manganese dioxide are also visual, doing a FESEM image comparison, shown in the figure 3.7. In this figure 3.7 is possible see a zoom of the surface of the electrode where, during the deposition, is create a "bubble". This happens because the solution is done by

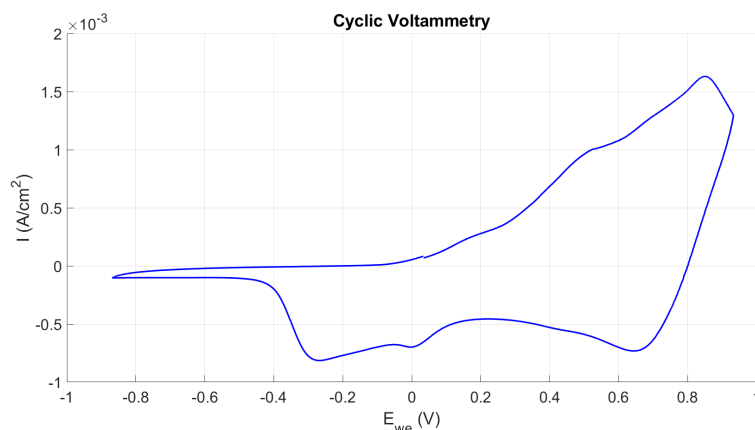


Figure 3.4: CV curve on the overall voltage window, from -0.9V to 0.9V. The used scan rate is of 5 mV/s and for each cycle the number of scans is of 20. The area of the tested electrode is of 1 cm^2 .

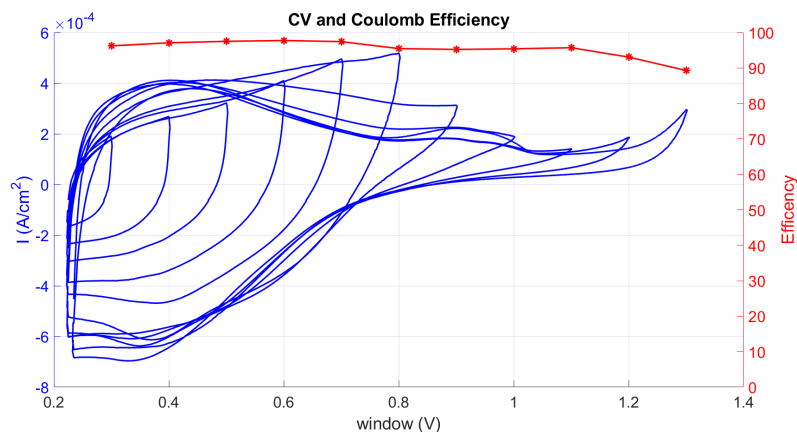


Figure 3.5: Superposition of different cycles of CV, from +0.1 V to +1.3 V, with the correspondingly Coulombic efficiency η . The used scan rate is of 5 mV/s and for each cycle the number of scans is of 20. The area of the tested electrode is of 1 cm^2 .

water and the potential applied is too high causing the electrolysis. These bubbles cause a not perfect uni-formation of the deposition, exposing the planar gold to the electrolyte: this can explain why the Coulombic efficiency doesn't reach the 99%.

	C (mF/cm ²)	ESR (Ω)
GOLD	0.9	1.7
MnO ₂	62	2.4

Table 3.1: Comparison of the density of capacitance, 'C', evaluated with the CV and the equivalent series resistance 'ESR', evaluated with the EIS, of the planar gold and manganese dioxide. The difference in capacitance is of a factor 69.

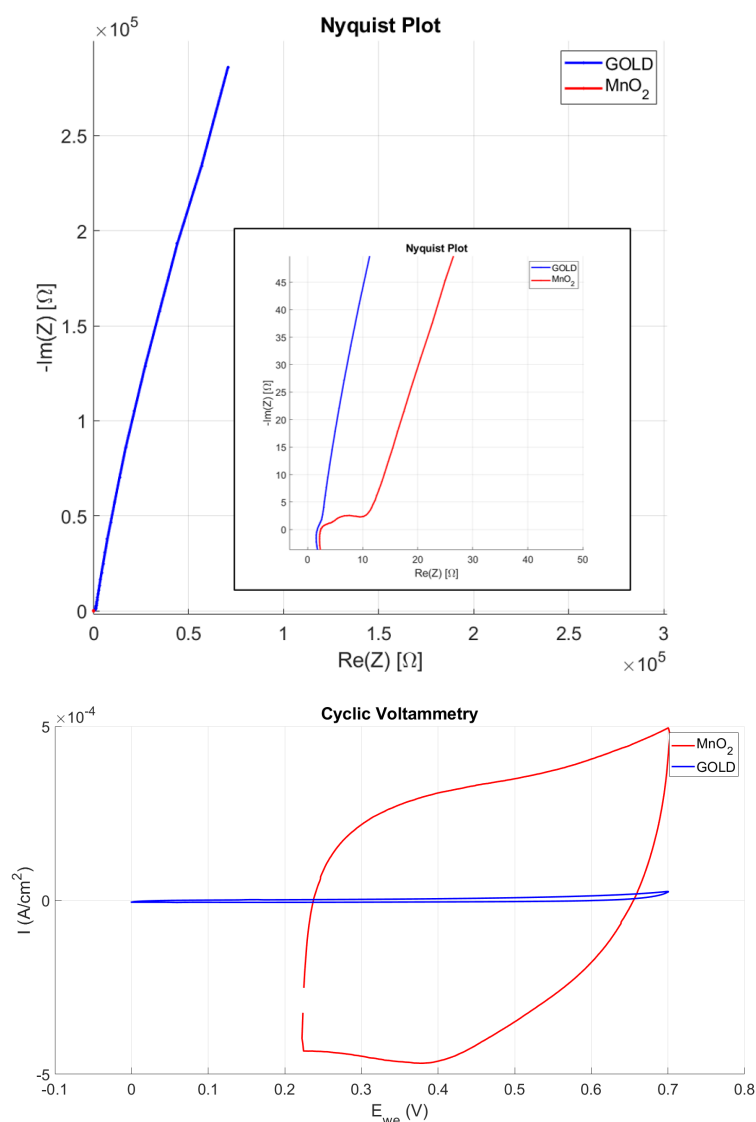


Figure 3.6: Comparison between the gold, red line, and the manganese dioxide, blue line. Above an EIS where is possible see how much the imaginary part of the two are different. At the bottom the superposition of different CV. Of course is possible see the visual difference between the two levels of current and so the big difference in term of capacitance. The two are both obtained with a scan rate of 5 mV/s and are the result of 30 scans, both with an area of 1 cm^2 . The only difference is OCP value starting point that is different for the two materials. The difference about the two values of capacitance is about a factor 69.

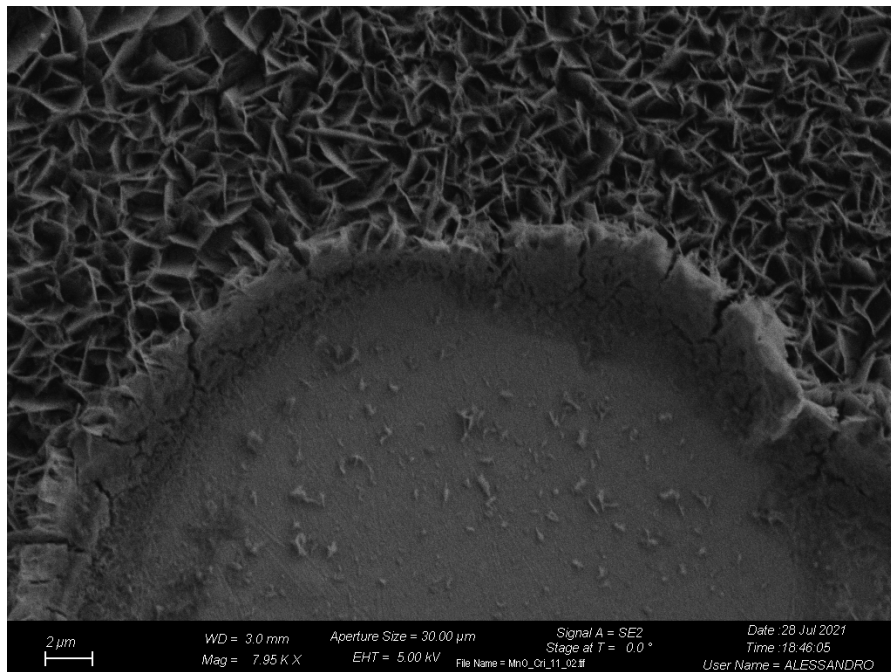


Figure 3.7: FESEM image comparison between planar gold and manganese dioxide. Above is present the MnO_2 and below the planar gold.

Chapter 4

Carbon-based electrode

The manganese dioxide works very well in the anodic potential window, but not in the cathodic. The other electrode need to be covered with other material, like the carbon-based materials, having the possibility to create an asymmetric device. Also in these case are used techniques in which the deposition is thanks the application of a current or a voltage to be replicated with planar devices.

4.1 EFD: Electro Phoretic Deposition

In Electro Phoretic Deposition (EFD) process, an electric field is applied between two electrodes that are dipped in a solution in which are suspended the carbon particles to deposit.

The carbon particles assume a negative charge when are put into the solution and for this reason in necessary apply the positive voltage into the electrode at which is wanted the deposition.

Also in this case, like in the electroplating, is first necessary find the correct set-up parameters to assure both a good adhesion than a good repeatability .

4.1.1 Colloidal solution

The first parameter to find is the composition of the colloidal solution in which are present the particles.

The solvent of this solution consists of water in which is present a 5 % w/w of ethanol. This because in literature the solution is completely done by similar type of alcohol [20] [21], but for cost and protection of the environment this is about totally replaced by the water.

On this is put a percentage of carbons that must be found. Five different percentages (w/w) of activated carbons, 0.5 %, 1 %, 2 %, 5 % and 10 %, are put in solution, observing the different behaviours. Each solution is put into the sonicator for 30 minutes to assure a good mix.

For the higher concentrated solutions of 5 % and 10 % the results are that they are too much concentrated so that the solutions begin to become solid.

For the 0.5 % instead, after small time, the carbons begin to precipitate.

The 2 % seems to be good, but during the time the high percentage of carbons begins to agglomerate and precipitate.

The 1 % seems to be the better and, for this, its near carbon concentration solutions are investigated. The solution in which the particles remain in suspension for more time without big formation of agglomerate is the 0.9 % of activated carbons. The type of carbons decided to test are the activated carbons. However their dimension are bigger compared by other type carbons. This could be relevant, because smaller particles can better attack on the porous surface of the 3D gold. To improve the solution two possible variants can be studied:

- carbons black: the idea is replace the activated carbons with smaller carbons as the carbons black,
- ball milling activated carbons. The idea is take the activated carbons and try to reduce their dimension using the ball milling technique.

The ball milling is a technique in which the particles are milled by balls. The carbons are put into a mill with steel balls. Thanks to magnetic force the balls are rotated and can mill the particles [22]. Depending by the dimension of the balls and their velocity so energy, is possible obtain different levels of milling. Is important however to consider that the balls can release some contamination, that can be seen with the a "ESD FESEM" analysis. This happens because the balls are done by steel, so a steel contamination is possible and was observed.

For this, the carbons are cleaned before the use with a Soxhlet extractor. The Soxhlet extractor is an instrument which aim is to reduce the quantity of impurities into the solute. The solute is put into a central chamber into a filter. Below, there is a chamber filled by water, that works as solvent, above a condensation chamber. The water is brought to the boil and then is condensed passing from to the central chamber, where there is the solute. Repeating this process is possible clean the solute saving the quantity of solvent because it is re-used [23]. To be sure of the result, another "ESD FESEM" analysis is done after the procedure, confirming the cleaning.

In the "characterization" section, it will be possible see the difference between these three difference choices of carbons: activated carbons, milled activated carbons and carbons black.

Doing some test with these solutions, is seen that the performance improve with the addition of a binder. The idea behind this is simply: the carbon's particles are negative. If in the solutions is put something of positive that could surrounded the particles, these can be work as a glue helping the adhesion at the electrode. Looking the positive ions, the $Mg(OH)_2$ can be used as binder and it is put in a concentration of one order of magnitude less of the percentage of carbons, so 0.09 %. Typically, the ethyl cellulose is used in literature as binder [20], in a concentration of 1:8 with respect to the carbons, for this is chosen to use this similar ratio.

4.1.2 Set-up

In the EFD the carbon's particles are deposited into the surface thanks to the application of an electric field. In literature is reported [21] that usually is needed an electric field of 100 V/cm to properly work.

The first set-up idea, shown in the figure 4.1, is put vertically the electrode and a planar titanium counter electrode of 0.75 mm into the solution, trying to bring them closer together, and applying a voltage.

The time of deposition depends by the behaviour of the current. In fact during the deposition the resistance increases because the carbons are deposited over the electrodes: applying a constant voltage, the current should decrease. This behaviour occurs until a plateau is reached above which the current is fixed, maybe because the deposition is saturated. Now is possible play with the distance, with the intensity of the voltage and duration to have the deposition. Because the electrode consists of thin layers, the most critical problem is avoid the delamination that can arrive when a too high intensity of voltage or field is applied. Is found that a voltage higher than 20 V put in a distance less of 5 mm creates problems of delamination. For this reason, is used 20 V at a distance of 5 mm creating for 10 minutes an electric field of 40 V/cm. This is less than the theory but seems to work. The main problem of this set-up is the not uni-formation of the deposition. Is impossible in fact avoid the meniscus that is formed between the air and the solution and in this the density of the field changes. Furthermore, when the electrode is pull down by the solution, the position if this meniscus varies and, especially in the final part, can create an higher deposition. These problems can maybe decrease losing area, so that the critical parts in which is present the meniscus can be deleted or trying to use more accurate instrument with respect to the arms to remove the electrode by the solution.

However, other possible set-up can be investigated as an horizontal set-up as shown in the figure 4.2. In this set-up the electrode in completely dipped into the solution: when this is vertically removed the meniscus is uniform at the whole surface and not only in a point creating different deposition.



Figure 4.1: EFD vertically set-up. On the left the result, comparing the electrode before and after the deposition, on the right the correspond set-up. In this latter, on the left is shown how to put the working electrode (yellow) and the platinum counter electrode (grey) into the colloidal solution (black). Between these is applied a voltage so that the electrode in which there is wanted the deposition is positive charged. On the right is shown an example of how the electrode will be. The deposition is not uniform and so, in the under part, the carbons are more present (more black color).

However also this set-up has problems because the electrode delaminates. It doesn't happens any times, but especially in the point at which is present the closer to avoid the loss of the solution, the contact is lost. In fact, how it is possible see from the figure 4.2, the electrode must be pressed so that the solution in the box doesn't loss. But this pressure with the application of the voltage, so a field and a current, destroys the device in that point. Also in this case, this problem can be solved, for instance changing the mode to come into the box. The box shown in the figure in fact presents a fissure in which the electrode is pinch-off, but bending the electrode is possible create a bridge so any fissure or pinch-off are needed. However, to limit the bending, a very long electrode and box are needed, losing areas and among of solution.

For both these techniques overall remains a big problem. These thin layers suffer of delamination process when are put in a big among of liquid how it happened also in the characterization of the current collector in a open cell. For this reason a

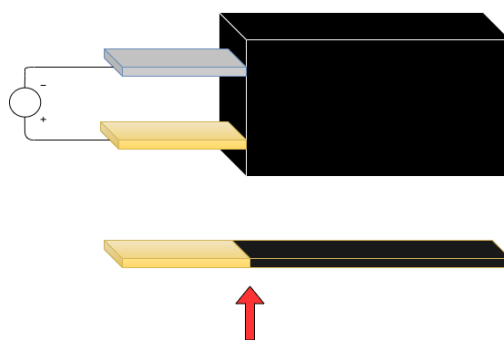


Figure 4.2: EFD horizontal set-up. Above is shown how to put the working electrode (yellow) and the titanium counter electrode (grey) into the colloidal solution (black). Between these, is applied a voltage so that the electrode in which there is wanted the deposition is positive charged. On the bottom is shown an example of how the electrode will be. The deposition is more uniform (black color), but the red arrow indicates the critical point at which happens the delamination.

third type of set-up is studied.

The idea is to limit the amount of solution in which are present the carbons to deposit to limit the delamination process.

On the electrode's surface is put a little amount of solution thanks to the help of a pipette. In the characterization section there are two examples of different quantities that produce different results. Then, using the needle of a micro-manipulator, is applied a field between this needle and the substrate as shown in the figure 4.3. Because with the vertical set-up is seen that a field of about 40 V/cm could be sufficient and because the distance between the electrode and the needle is less than 1 mm, is chosen to apply a field of 3V, recording a current of a few hundred of μA .

The advantages of this technique are:

- the amount of solution is precise so, knowing the concentration, is known the amount of deposited carbons. With the previous technique the only possibility is weigh the samples before and after the deposition, but because the weight of the particles is very very small, the accuracy of the measuring instrument is on the same order of the deposited material and so is not very accurate,
- the amount of solution is very small so no delamination process are present also with field higher of 40 N/cm,
- because the process is well controllable, it is also repeatable.

However are present also disadvantages like:

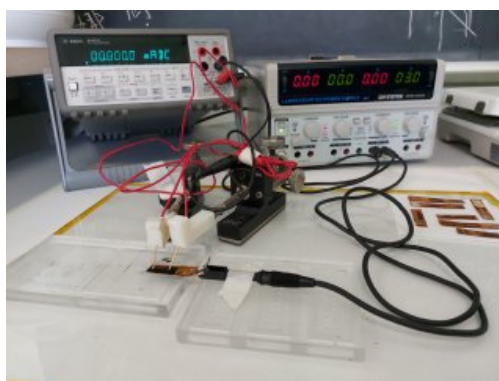


Figure 4.3: Photo of the set-up for the EFD. In the foreground is present the sample between which is applied a field. In the background, on the left an amperometer to measure the current, on the right a voltage source to generate a voltage.

- uni-formation of the deposition. From a practice point of view, the absence of a meniscus, makes deposition more uniform than the vertical set-up. However, in theory, because the field is generated from a needle and not from a plane, the field is radius and so less uniform. To overcome this problem is possible apply more needles, but of course they can not be as a plane,
- this technique is not properly an EFD process, but seems to be a precipitate deposition. However is possible compare the difference performance between the applying or not of a field to understand if this process could be seen as an EFD process or simply a precipitation process,
- this technique with respect to the other is more difficult to apply in a industry fabrication process.

However, looking to the results, this technique for the deposition of carbons seems to be the best between these three and for this is used.

4.1.3 Characterization

Once that the colloidal solution and the set-up are defined, is necessary create the electrodes and characterize them.

Putting $50 \mu\text{l}/\text{cm}^2$ of solution on the electrode and applying a voltage of 3 V for 30 minutes, is obtained the CV results shown in the figure 4.4. This time is chosen for two reasons: the first is that after 30 minute the solution begins to pass from liquid to solid state at 20°C and the second is that the current stabilizes in this time.

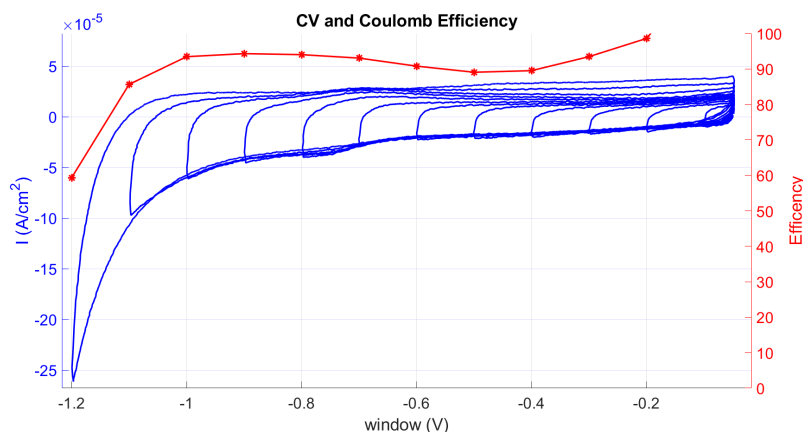


Figure 4.4: Superposition of different cycles of CV, from -0.1 V to -1.2 V, with the correspondingly Coulombic efficiency η . The used scan rate is of 5 mV/s and for each cycle the number of scans is of 20. The area of the tested electrode is of 1 cm^2 .

From this CV results is possible see that the maximum voltage window is of -1V. Under this value the Coulombic efficiency begins to decrease and doing more scans for voltage of -1.1V or -1.2V is possible see a decrease of this efficiency during the time.

So the maximum voltage window for the cathodic electrode covered by carbon black is of -1V. Looking at the capacitance, however, is seen a very low density of capacitance of about 4 mF/cm^2 . This low capacitance can be caused by a small amount of carbon put over the electrode. Because it is small, also the duration of the application of a field is small and so could be not sufficient for the EFD. For this reason, the amount of solution put over the electrode is increased until the broken of the meniscus, that happens just above the 65 $\mu\text{l/cm}^2$. With this quantity, the application of the field can be extended for one hour. The CV results are shown in the figure 4.5.

This time the tested voltage windows are not from -0.1 V, but around the found -1V, so from -0.9 V to -1.2 V. Decreasing the number of windows and having the same measurement's time of the figure 4.4, is possible increase the number of scans from 20 to 30, using the same scan rate of 5 mV/s. The Coulombic efficiency is high above of 99 % until -1 V, taking the value of 98 % at -1.1 V and reaching the 96 % at +1.2 V. For this reason, is chosen as maximum windows -1 V. About the density of capacitance, it is of 28 mF/cm^2 .

If it is considered that the substrate is of 3D gold, the increase of the capacitance is very high, by a factor 16, as it will possible see into the figure 4.6.

To understand if the application of a field is significant or not, is done a

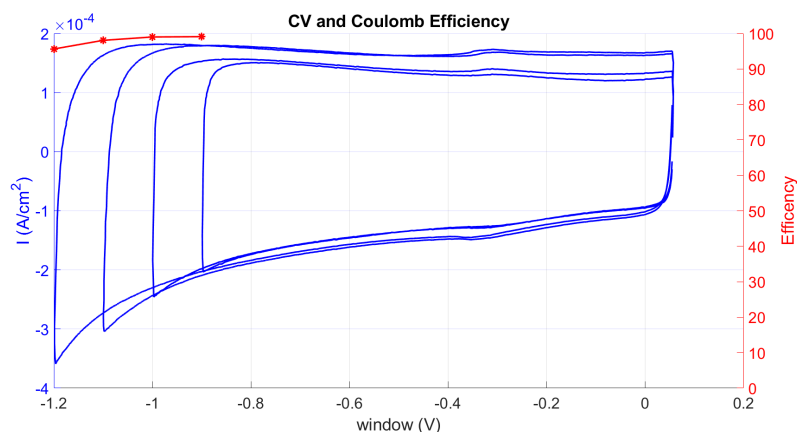


Figure 4.5: Superposition of different cycles of CV, from -0.9 V to -1.2 V, with the correspondingly Coulombic efficiency η . The used scan rate is of 5 mV/s and for each cycle the number of scans is of 30.

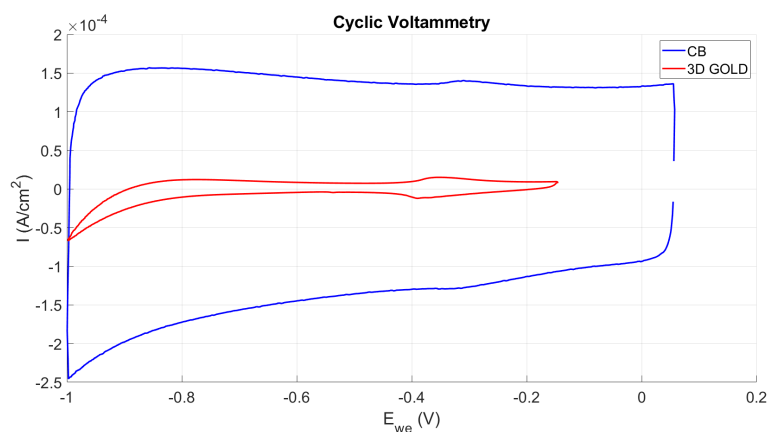


Figure 4.6: CV comparison of the carbons black, blue line, with respect to the 3D gold, red line. The area is for both at 1 cm^2 , while the scan rate is of 5 mV/s.

comparison of carbons black between a deposition for precipitation and a deposition with the application of a voltage. The EIS Nyquist plot results are shown in the figure 4.7.

The left part of the figure 4.7 seems to show only the behaviour of a precipitation deposition: in reality there is also the behavior with the application of the field, as demonstrated the right part, but the difference is so high that the blue line seems to disappear. From this, is possible derive that for the EFD the capacitance is of 28 mF/cm^2 with a ESR of 1Ω , while for the precipitation method the capacitance is of 1.4 mF/cm^2 with a ESR of 1.9Ω . The same carbons with the same quantity

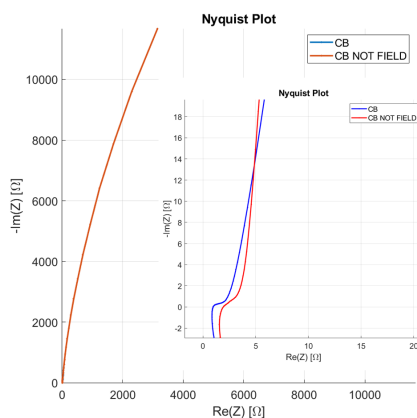


Figure 4.7: EIS comparison between the CB applied with a voltage, blue line, and without, red line. The two plots are the same: on the left there are the line correspondingly to all the frequency, from 10 mHz to 1 MHz, instead on the right there is a zoom of the higher frequency. The area of all the tested electrodes is of 1 cm^2 .

produce a difference of a factor 20 in the capacitance.

Also comparing the CV is possible obtain the same results as shown in the figure 4.8.

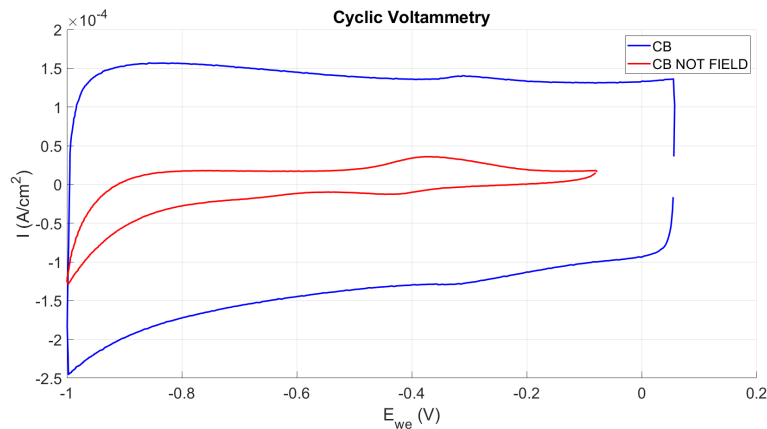


Figure 4.8: CV comparison between the CB applied with a voltage, blue line, and without, red line. The application of a voltage is of -1 V for the both and the used scan rate is of 5 mV/s.

From the figure 4.8, is possible immediately see that the capacitance applying a field is better and the summarized results are shown into the table 4.1.

The first value of capacitance is little bit different with respect to the value

	C (mF/cm ²)	ESR (Ω)
EFD	28	1
PRECIPITATION	3.6	1.9

Table 4.1: Comparison of the density of capacitance, 'C', evaluated with the CV and the equivalent series resistance 'ESR', evaluated with the EIS, of the two deposition methods. The Electro-phoretic-deposition have better parameters with respect to the precipitation methods.

found in the EIS. However, the EIS' capacitance is not so precise, but do only an idea of the order of magnitude that is coherent with the result.

Considering the carbon's materials that can cover the electrodes, as said, there are two possibility: the carbons black, CB, and the activated carbons, AC. The two present difference about the process to derive them, but also about the dimension of the particles and the porosity. In fact, the AC present an higher surface-area-to-volume, presenting an higher porosity. From this, seem to be the best both for the deposition on the electrode and for the link with the electrolyte's ions. However, as said, their dimension is much higher with respect to the CB, having particles of some micro-meters size [24] with respect to the nano-meters of the CB [25].

A smaller dimension can increase the match with the porosity of the 3D gold, helping the deposition. Because the AC have an higher dimension, they can be milled with the Ball-Milling technique. To do this, 30 ml of AC are put into a crucible of 80 ml and the process is carried out with steel balls for 2 hours.

The three different carbons, the carbons black, activated carbons and ball-milled activated carbons are tested and compared to understand which is the best.

In the figure 4.9 is possible see the Nyquist plots of these.

From this, are possible derive that the CB produce a capacitance of $28mF/cm^2$, the AC of $12mF/cm^2$ instead the AC BM of $19mF/cm^2$.

From these data is possible derive that the carbons black is the best. However the ball-milling produces an improvement of the activated carbons. This result could be say that if the particles are further decreased, the AC can produce an higher capacitance.

Also a CV analysis is done and the results are shown in the figure 4.10.

From these results is possible obtain the table 4.2. Looking these results is possible see a different behavior of the Ball-milling AC: with this measurement the capacitance seems to be of $38 mF/cm^2$ and not of $19 mF/cm^2$. This behavior

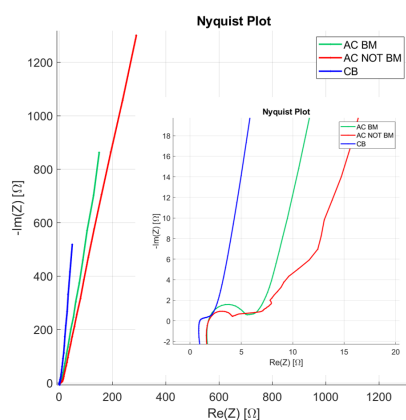


Figure 4.9: EIS comparison between the carbons black 'CB', blue line, the activated carbons obtained with the Ball-Milling 'AC BM', green line, and without the Ball-Milling 'AC', red line. The two plots are the same: on the left there are the line correspondingly to all the frequency, from 10 mHz to 1 MHz, instead on the right there is a zoom of the higher frequency.

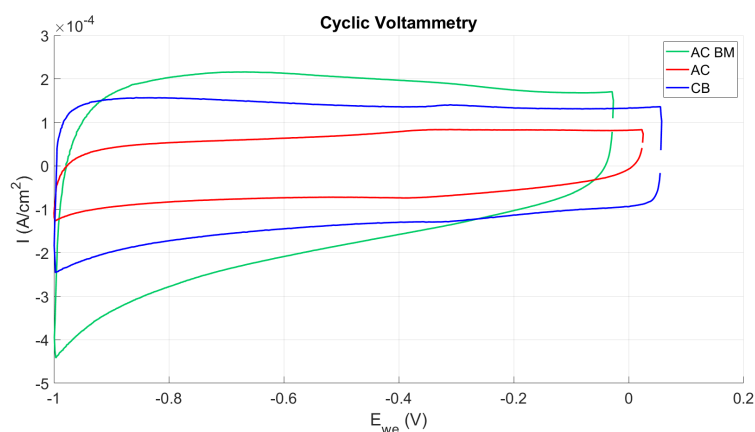


Figure 4.10: CV comparison between the CB, AC BM and AC. The application of voltage is of -1 V for the both and the used scan rate is of 5 mV/s.

could be explained considering that the EIS is done before the CV. During the application of a voltage, there could be an activation process of the surface that increases the capacitance. This is explained also considering that for each window the number of scans is not set to one because is need a stabilisation, during the which the efficiency and the capacitance increases. For this reason is better do an EIS also after the CV to be sure of these results.

	C (mF/cm ²)	ESR (Ω)
AC BM	38	1.8
AC	13	1.8
CB	28	1

Table 4.2: Comparison of the density of capacitance, 'C', and equivalent series resistance 'ESR', of the three carbon based-materials. The capacitance is obtained with a CV, instead the ESR with an EIS. The ball-milling AC have the best performance between the three.

From this is so possible see that the AC BM are the best material to deposit. However, the creation of the AC BM takes time because is necessary to do the ball milling technique and then the cleaning. To save time it is chosen to use the carbons black, however from these results, to have an increase of the performance is better used the AC BM.

The final comparison that is shown, is between the carbons based material and the manganese dioxide for what concerns the anodic potential window. As seen in the previous chapter, the manganese dioxide is not good for the cathodic window so it was necessary find and analyse a new material as the CB. However this does not mean that the CB can not be used for the anodic window. Doing some trials in fact, what is found is that the CB can work also in the anodic window, but has a worse performance. It presents a lower potential windows of +0.4 V instead of the +0.7 V of the MnO_2 , and the different density of capacitance and efficiency are summarized into the table 4.3.

	C (mF/cm ²)	η %
CB	23.5	84
MnO_2	34.1	97

Table 4.3: Comparison of the density of capacitance, 'C', and Coulombic efficiency ' η ', of the CB and MnO_2 at +0.4 V. How it is possible see, the MnO_2 is the best between the two.

Because the efficiency and the capacitance are better for the MnO_2 , this explains why is chosen this material for the anodic window.

Chapter 5

Asymmetric stack device

5.1 Realization of an asymmetric device

The two previous chapters shown the behavior of different materials into the aqueous electrolyte. In the cathodic window, the behavior of the CB is better, like as into the anodic is better the behavior of the manganese dioxide. These results have produce a cathodic potential window of -1 V with a density of capacitance of 28 mF/cm^2 and an anodic potential window of +0.7 V with a density of capacitance of 62 mF/cm^2 .

If there is considered the Coulombic efficiency, is possible see that the anodic and the cathodic windows have two different threshold's values. In fact for the cathodic is chosen as threshold the value of 99% instead for the anodic 97%. This is done because the Coulombic efficiency is perfectly stable until a certain voltage, above which begins to decrease: exactly this value of voltage is set as the maximum. For the cathodic window, is correct set at threshold of 99%, but for the anodic in theory also in this case should be set at 99%. As said the manganese dioxide however does not cover perfectly the gold that can be exposed to the electrolyte due to the "bubbles" of the electrolysis: the Coulombic efficiency of only the planar gold is not very high, about the 62 %. Overall, is so correct that the efficiency is not of the 99%, because it is not characterized only the manganese dioxide. For this reason is necessary change the threshold changing it from the cathodic to the anodic. The figure 5.1 summarizes these results.

Taking the equation 2.1, is possible derive the charge Q as in the equation 5.1:

$$Q = C \cdot \Delta V = C_D \cdot A \cdot \Delta V \quad (5.1)$$

where ' C ' is the capacitance, ' C_D ' the capacitance's density, ' A ' is the area and ' ΔV ' the applied voltage window. The idea behind an asymmetric device is create a device that can store the same charge at both the electrodes.

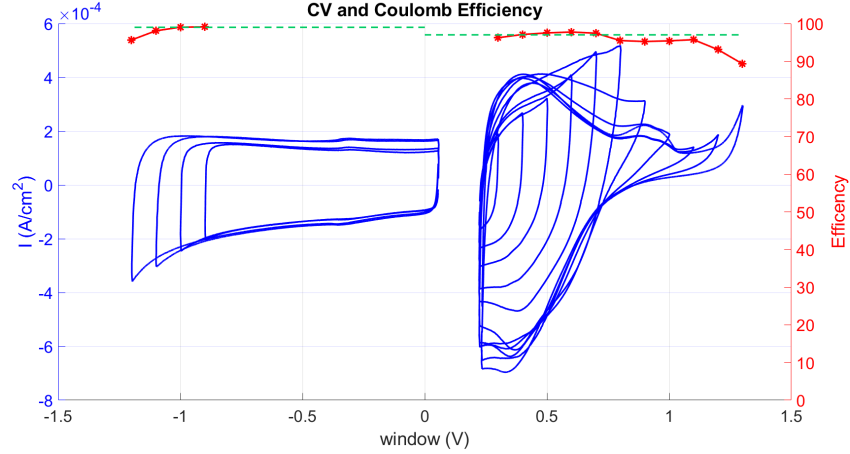


Figure 5.1: Superposition of the anodic CV, with the MnO_2 , and the cathodic CV, with the CB, in blue. The red line shows the Coulombic efficiency correspondingly at the voltage windows. The dot green line is set at 97 % for the anodic, and at 99% for the cathodic.

Because ' C_D ' and ' ΔV ' depend by the interaction electrode's material with the electrolyte, the only possibility is change the ratio between the two areas. What is obtained is the equation 5.2:

$$\frac{A^+}{A^-} = \frac{C_D^- \cdot \Delta V^-}{C_D^+ \cdot \Delta V^+} \quad (5.2)$$

Replacing the values of the parameters in the equation 5.2, is possible obtain a ratio of:

$$\frac{A^+}{A^-} = \frac{28mF/cm^2 \cdot 1V}{62mF/cm^2 \cdot 0.7V} = 0.65 \quad (5.3)$$

This means that to have the optimal Coulombic efficiency, the two areas must be in ratio of 0.65. For this reason, a stack device is tested with this ratio.

5.2 Measure's results

Thanks to the previous results is possible create the asymmetric device.

The device is closed into a stack configurations, that means that the two electrodes are one in front of the other. In between there is the fiber glass filled by $500 \mu l$ of $1M Na_2SO_4$. The anodic electrode of MnO_2 has an area of $1 cm^2$, instead the cathodic electrode of carbons black has an area of $1.6 cm^2$. The overall cell is closed into a pouch cell and is tested with a two electrodes measurement, putting

the two contacts of titanium grid on the two electrodes.

The EIS results is shown in the figure 5.2

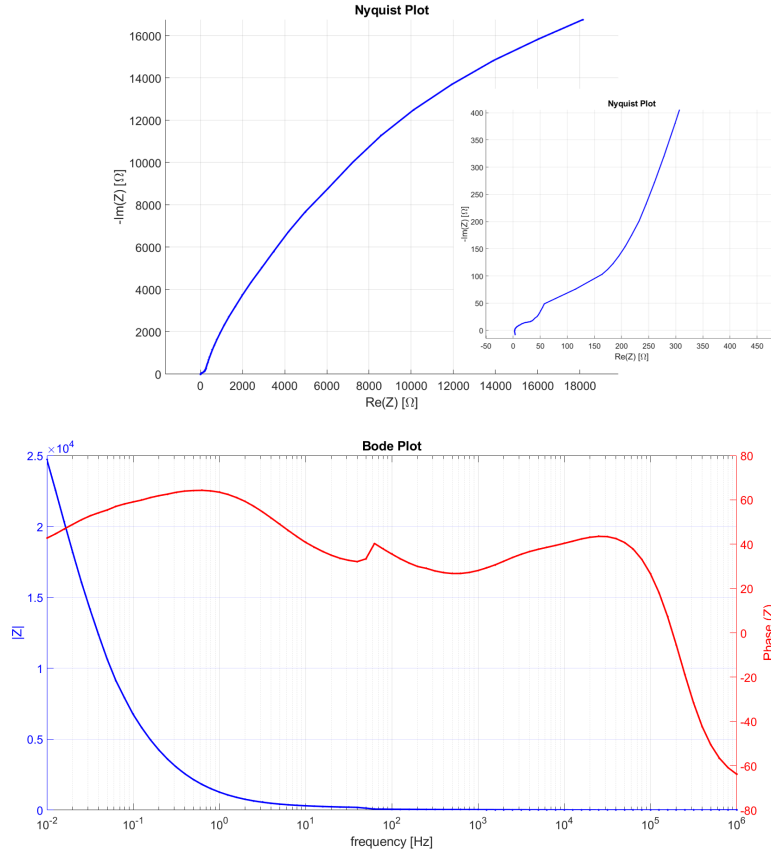


Figure 5.2: EIS graphs results of an asymmetric stack device. Above there is the Nyquist plot: the two images are the same, the left is with the full axis, the right is a zoom at high frequency. Above the correspondingly Bode plot.

From these results, is possible see a ESR of 2.7Ω . Then the CV analysis is done with a scan rate of 5 mV/s .

From the figure 5.1 what is possible see it that for the anodic the maximum voltage is of $+0.7 \text{ V}$ starting with an OCP value of 0.2 V instead for the cathodic the maximum voltage is of -1 V starting from $+0.06 \text{ V}$. This means that the overall voltage that can be applied at the cell is of : 5.2

$$\Delta V = (0.7 - 0.2) + (0.06 - (-1)) = 1.56V \quad (5.4)$$

For this reason, the cell is brought at 1.6 V . The CV result is shown in the figure 5.3.

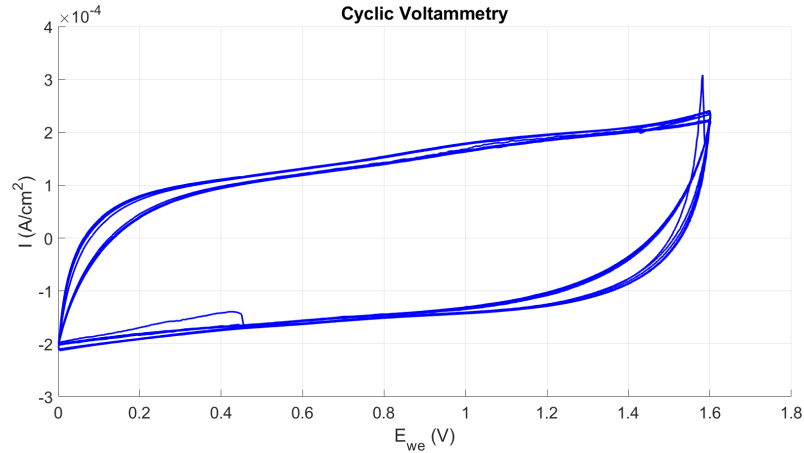


Figure 5.3: CV of asymmetric stack device consisted of an anode electrode of MnO_2 and a cathode electrode of CB. The ratio between the two areas is of 1.6, the first has an area of 1 cm^2 the second of 1.6 cm^2 . The used scan rate is of 5 mV/s and the scans are of 30.

Thanks to the CV results is possible calculate a capacitance density of 25 mF/cm^2 taking as areas the bigger, so the area at 1.6 cm^2 and a correspondingly Coulombic efficiency of 97% .

The device is tested also with a CCDC after 3 days from the CV measure. The set-up for this analysis is a set of five different ranges of current: $50 \mu\text{A/cm}^2$, $100 \mu\text{A/cm}^2$, $200 \mu\text{A/cm}^2$, $500 \mu\text{A/cm}^2$ and $750 \mu\text{A/cm}^2$ and for each is set 50 scans. The correspondent Rate Capability plot is shown in the figure 5.4.

In the figure 5.4 is possible see only the range of current in which the device works well that are only the slow range of current. The ranges of $500 \mu\text{A/cm}^2$ and $750 \mu\text{A/cm}^2$ instead are too high for this device and for this are cut. About the values of capacitance, this is a little bit different by the values found with the CV: because the measure is done after 3 day maybe the device stabilised producing these results. In this case the capacitance is evaluated from the square of the charge dividing for the discharge energy multiply by a factor 0.5. Is chosen the discharge energy instead of the charge because the discharge is effectively the energy that the device can release.

Considering only the ranges of current in which the device produce a capacitance different from zero, is possible also obtain the GCD profile shown in the figure 5.5.

Thanks to the figure 5.5 is seen that the shape is the typical triangular shape of a SC, having also the characteristic of the pseudo-capacitance that rounds up the triangle. Increasing the current density, the IR increases as is possible see passing

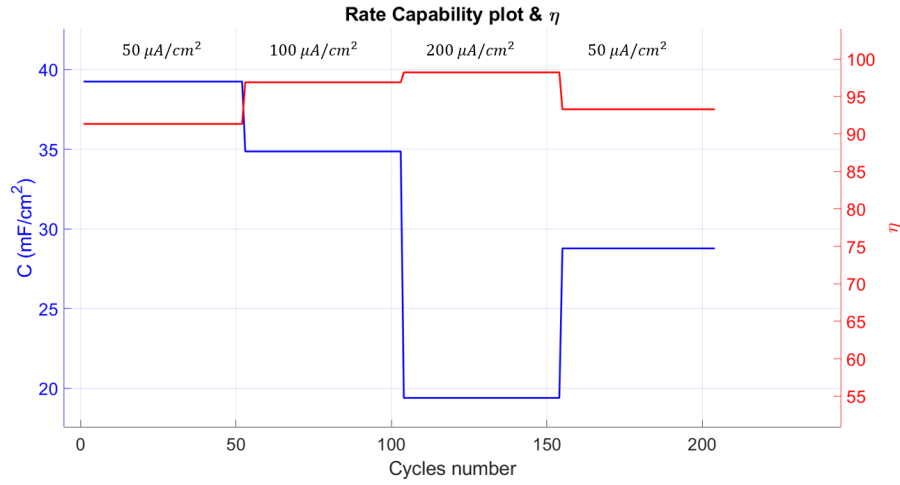


Figure 5.4: Rate capability plot. On the y axis is present the density of capacitance instead on the x axis is present the number of cycles. In this figure are cut the ranges in which the device doesn't work.

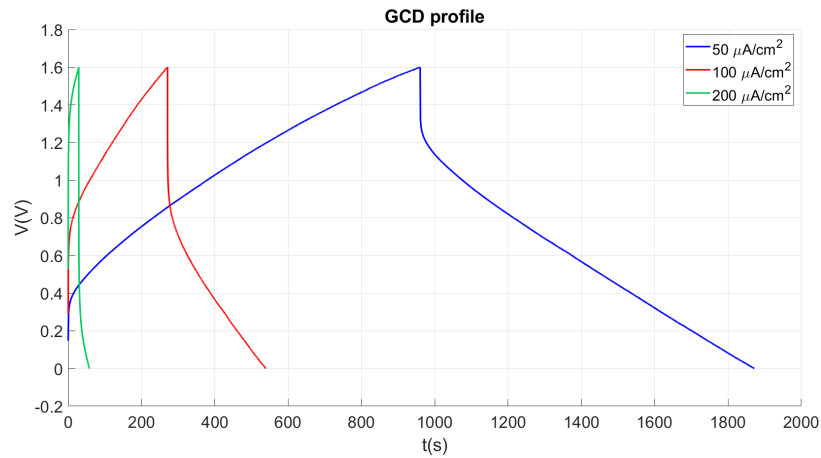


Figure 5.5: GCD profile referred to three different range of current. Increasing the range is possible see that the IR drop increases.

from the blue to the green line.

Finally is also possible evaluated the Ragone plot shown into the figure 5.6. On the y axis is shown the discharge energy for the same reason explained above, instead on the x-axis is present the power density evaluated as the discharge energy divided by the discharge time, all divided by 1.6 cm^2 . In this figure are also present references with the literature. In this last graph is possible see the different applications of the tested device: thermo-electric and mechanical harvester [26].

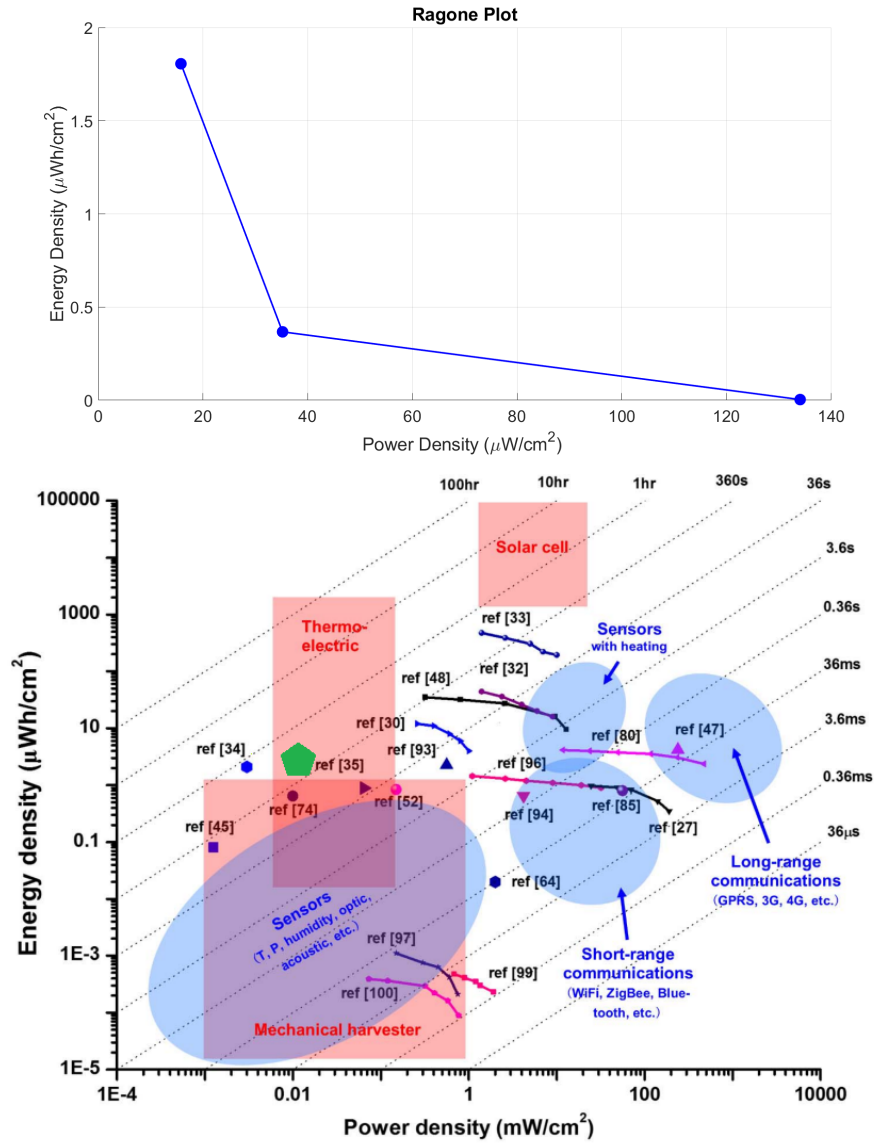


Figure 5.6: Ragone plot. On the y-axis is the energy density and on the x-axis is the power density. Above are shown the experimental results of the asymmetrical device. Below are references to the literature where the green pentagon represents the tested device [26].

Chapter 6

Planar device

6.1 Introduction

The device described in the previous sections is a device assembled in a stack configuration, where the two electrodes are one in front of the other. This device works well, however also a planar configuration is tried to study to create effectively an integrated μSC .

As said into the introduction chapter, a planar device is a device in which one dimension is completely absent and in which the two electrodes could be put very near also creating different electrode's layouts to try to increase the capacitance. With this idea was born the so called "interdigitated" layout, where increasing the interface between two electrodes, increases the capacitance.

In this thesis project, a lot of work is done versus the creation of these kind of devices, however the results produced are not so good as the results had with the stack configuration. Nevertheless some steps in this direction are reached. First of all, the techniques chosen in the previous sections are chosen because applicable at the planar devices. Secondly, different from the stack, before the electroplating and the EFD, the device is successfully modeled with photographic process to create the correct layout. To characterize the planar materials, is necessary a three electrodes measurement and in this direction will be shown future possible developments because it is the most critical point to achieve. Finally, in this chapter there will be shown a prototype with the correspondent capacitance and efficiency compared to the stack configuration.

6.2 Photolithographic process

To create a planar device there are different possible layouts. The layout may vary from two easy electrodes with the same area put placed side by side to a more

complex shape. The overall studied shape are shown into the figure 6.1.

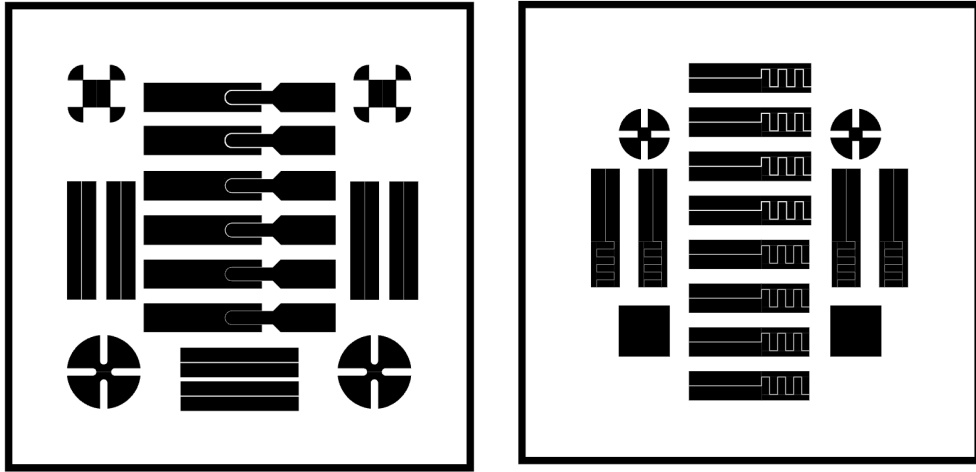


Figure 6.1: Example of two masks produced for the creation of planar devices. The devices are in the middle, instead in the corners there are examples of layouts used for the measure of the sheet resistance, used for the evaluations of the thickness of the substrate.

A substrate of $10 \times 10 \text{ cm}^2$ of kapton, chromium and planar gold is produced with an evaporation process. Then this square sheet is brought into a clean room of class 100. Here on the substrate is started a photographic process.

The main steps of this are :

- cleaning of the substrate with ethanol,
- deposition of the photo-resist with spin coating,
- soft bake: evaporation of the solvent of the photo-resist at $100 \text{ }^\circ\text{C}$ for 1 minute,
- exposure to the UV source (figure 6.2),
- development of the photo-resist,
- hard bake of the photo-resist at $100 \text{ }^\circ\text{C}$ for 1 minute,
- etching of the gold for 2 minutes,
- etching of the chromium for 5 minutes,
- removal of the cover photo-resist with acetone.

The used photo-resist is a positive photo-resist: taking the masks shown into the figure 6.1, the photo-resist after the development remains in the "black" zone of the masks. This resist protects the under layers of gold and chromium that will not be etched, so the final devices will be exactly as appear into the masks. These devices have an overall working area of about 1 cm^2 , summing the areas of both the electrodes. In the showed masks, the device are bigger because are present also the contacts to avoid the titanium's grids. For what concerns the distance the two electrodes are in a different distance of $100 \mu\text{m}$, $200 \mu\text{m}$ and $300 \mu\text{m}$.



Figure 6.2: Set-up of the photolithographic process with the UV source, into a class 100 clean-room.

6.3 Characterization of each electrode

To create an asymmetric planar device is necessary find the potential windows and the capacitance. The first depends by the temperature, that is constant, and by the interaction between electrode and electrolyte, that is the same used for the stack configuration, instead the second depends by the geometry of the device. For this reason is necessary repeat the steps done for the stack device. Looking a the figure 6.3 is possible see that to correctly characterize each electrode is necessary start with a three electrodes characterization, but passing from a stack to a planar configuration the position of the reference must be changed.

The best solution of this problem is transform one of the two electrodes of the device into a reference electrode, as shown in the figure 6.3. As said the $\text{Ag}|\text{AgCl}$ works well into the aqueous electrolyte, however is not so easy to evaporate on a kapton substrate, leaving aside the cost.

Remembering that the main characteristic of a reference electrode is an unchanged voltage drop during the time of the measure, if one material has the same characteristic it could be used as reference electrode.

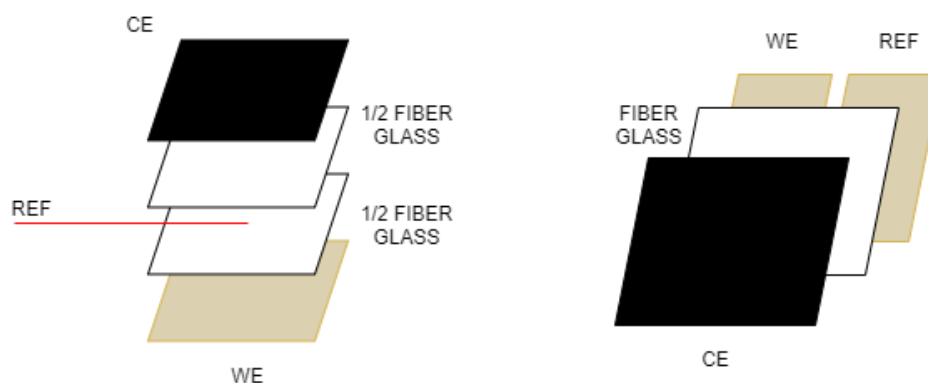


Figure 6.3: Different set-up for a three electrodes measurement. On the left there is a stack configurations where the working electrode (WE), the reference (REF) and the counter electrode (CE) are put one each above the other because the reference is a wire so is possible. On the right instead a planar configuration where the reference and the electrode are in the same plane and above are put the fiber glass with the counter-electrode.

Looking to the circuit component of the Autolab's instrument measurement, is possible see that the output of the reference electrode is the input of an operational amplifier. This means that the current that passes across the reference electrode is the off-set current of an operational amplifier, so in the order of the nA. Looking at the formula 1.1 is possible obtain the variation of the voltage into the time inverting it, and obtaining the equation 6.1:

$$\frac{\Delta V}{\Delta t} = \frac{I}{C} \quad (6.1)$$

This means that if the electrode material has an high capacitance, due for instance by an high superficial area and if it is crossed by a small current, like into the reference electrode, the variance in the time of the voltage is very small.

For this reason has tried to put as reference electrode an amorphous layer of 3D gold and then of carbons black. Considering a capacitance of some mF and a current in the order of the nA, the variance of the voltage should be in the order of the $\mu V/s$ so very low.

Many trials are done with different geometries, trying to changing the reference electrode to find the best that assures a stabilization. The main problems about these measures are the repeatability and the results obtained. In fact, the Coulombic efficiency is not stable during the scans and during the different voltage windows, creating problems for the definition of thresholds to find the maximum windows. Furthermore, the carbons black electrode could be used as reference for the characterization of 3D gold (although in reality the measurements made do not produce

repeatable results), but to characterize the carbons black is used as reference the same material, so there isn't the difference in capacitance, because are the same. Same consideration could be done taking the manganese dioxide as reference. Because of these problems, to do a correct set of measures is necessary find a third material that has or a very high value of capacitance or is stable in 1M Na_2SO_4 as the Ag|AgCl. In the 'further development' section could be shown a solution for this.

6.4 Creation of the device

In the characterization section is shown that to correct characterize an electrode is necessary introduce a third material that could be used as reference. Without a correct characterization, the planar device that will show in this section consists by two equal areas, just to have an idea of how much the results change with respect to the stack configuration.

To create the device is first of all necessary define the order of the sequence of processes.

The 3D deposition of gold is the best deposition: it is very well attached to the surface and doesn't release quantity of material when is put into a solution. Because the melting point of the gold is of 1185 °C, in theory this could be put into the "Büchi" at 300 °C. For this reason is chosen to use this as first process, then the electro-plating of the manganese dioxide and finally the EFD. The latter in fact is the more weak, so it not convenient further stressed it choosing to do this at the beginning.

Doing this sequence however is impossible deposit the carbons black because the surface of the 3D gold became completely hydrophobic after the calcination process. Although the gold is far by its melting point, the calcination process maybe reduced it, making porous gold no longer a substrate for the carbon deposition.

For this reason, the correct used sequence is start with the deposition of the manganese dioxide, then create the 3D gold and finally the carbons black deposition.

6.4.1 Results

The tested planar devices are the two showed into the mask on the left of the figure 6.1. The distance between the two electrodes is of 300 μm and 100 μm . The devices shown in the middle of the mask is called "one digit", with a distance of 100 μm instead the device composed by two parallel electrodes take the name of "planar", with a distance of 300 μm . To have an idea of how appears visually the final device, into the figure 6.4 is shown a photo.

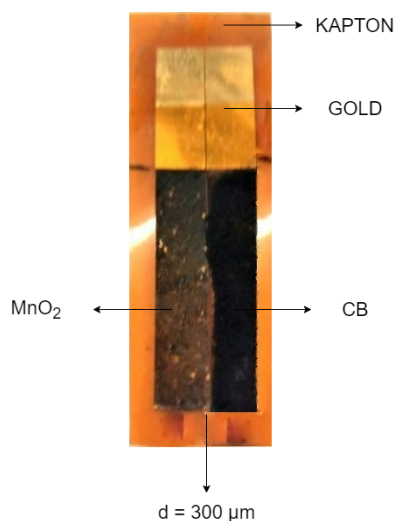


Figure 6.4: Planar device results. On the left is possible see the manganese dioxide, while on the right there is the carbons black particles. The two electrodes have a distance of $300\mu\text{m}$.

The balancing of the areas assure to maximise the potential window. Because with the balance the potential is of 1.6 V, this means that of course is impossible obtain the same value with the same areas. If the voltage is set too high, one potential drop could be overcome its limits with the consequence creation of reactions.

It is experimentally seen that a voltage of +1 V don't produce unwanted phenomena. Is important to notice that the following results don't show that the maximum potential window of a symmetric planar device is of 1 V, but only show the difference between two different kind of planar devices comparing with a stack configuration a +1 V.

The figure 6.5 shown the comparison between them.

From these results is possible obtain the following table 6.1.

	C (mF/cm^2)	η %
Stack	11.34	97
Planar	3.67	25
One digit	2.24	28

Table 6.1: Comparison of the density of capacitance, 'C', and Coulombic efficiency ' η ', of the two tested planar devices, one digit and planar, with the stack device.

From these results is possible see that of course the performance of the stack

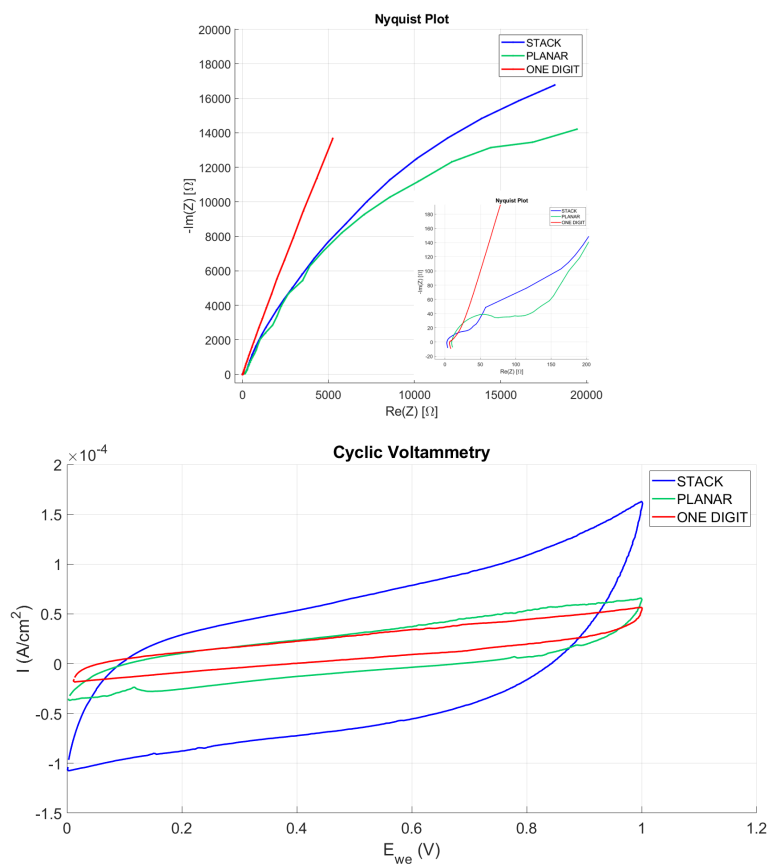


Figure 6.5: Planar device and stack comparison results. Above there is the EIS and below the CV comparison. The blue line represents the stack device with an area of 1.6 cm^2 , the green line the two rectangular electrodes planar put in a distance of 300 cm^2 and with an area of 1.54 cm^2 , while the red is the planar one digit with an overall area of 0.87 cm^2 and which electrodes are separated of $100 \mu\text{m}$ of distance.

device are better. However, only the stack device has a constant efficiency and constant capacitance so only for this device the above results have a meaning. For the planar what is possible see is a net decrease of the value of capacitance and a net decrease of the Coulombic efficiency.

Chapter 7

Conclusions and future developments

7.1 Conclusions

The SC is an energy storage device that recently has been studied a lot. The work of this thesis has made possible the realisation of a physical stack device that can work with aqueous electrolyte. The needed of integration leads to the scaling down of the device creating the μSC where the "micro" term meaning that the two electrodes are separated by a distance into the micro-metric scale. Thanks to the characterization section, as been possible study the behavior of different electrode's materials into the aqueous electrolyte, finding the limits and trying to minimize them as possible. Thanks to this latter aim, the created device is asymmetric both for the chosen of materials both for the ratio of the areas. In fact once that the materials are found, is necessary optimize the area to increase the potential window. To create the electrodes a lot of different deposition techniques are studied, from the evaporation, to the electroplating and electrophoresis trying to find the best set-up parameters for all.

In parallel to this, is studied also the closer of the cell, the creation of the reference and counter electrode and not only a single layout, but different passing from to stack to the planar.

The final result is an asymmetric stack SC, which positive electrode consists of manganese dioxide while the negative consists of carbons black and which area's ratio is of 0.6. The distance between the two electrodes is of $675 \mu m$ that is the thickness of the fiber glass, but choosing another fiber glass it could be possible decrease it. This device can work into a 1M of Na_2SO_4 until 1.6 V, producing a capacitance of $25 mF/cm^2$ and with a Coulombic efficiency of 97 %.

Finally, also a planar configuration is analyzed, creating masks and doing photographic processes. With this layout is effectively possible create μSC with a distance of the electrodes of $100\mu m$. In this case however, the device is still under study and in the following section are shown some trials that can be done to improve it.

7.2 Future developments

In this section are present possible developments that can be useful to optimize the device described above. These trials are summarized in the following subsections for simplicity.

7.2.1 Deposition techniques

The parameters for the deposition techniques described in this thesis are experimentally found, and maybe are not the only that can assure a good results.

For what concern the electroplating of the 3D gold, is possible analyze what happens when the time is decreased, playing between a time of 50 s to 420 s. This because after 50 s the 3D gold begins to grow and in this work the process is stopped after 7 minutes. Maybe decreasing the time, the deposited mass of 3D gold decreases but remains sufficient to assure a good substrate for the carbons materials. This could be useful because the manganese dioxide electrode will be put into the electroplating gold solution and so same contamination of release of material could be possible, but these possibilities decrease with the decrease of the contact time.

Also for the electroplating of the manganese dioxide the time can be decreased, because is done a trial of deposition of only 5 minutes (the used in this thesis is of 60 minutes) and something it is deposited, but is necessary test it to understand if the capacitance is sufficient. A less duration in this case could decrease the stress. Additionally, a less thickness of the MnO_2 can decrease the resistive effect seen during the EIS analysis.

To improve the uni-formation of the manganese dioxide instead could be useful avoid the electrolysis of the water that creates the bubbles over the electrode. To do this, is possible increase the distance between the two electrodes from 2 to 4 cm for instance, and see if there is again a deposition with a similar capacitance but with less bubbles that create a non uni formation.

For the EFD is possible play with the adding of the methyl cellulose as binder to see if the attack of the carbons increases. This technique is, in fact, the most fragile, and to increase the adhesion is possible play with the colloidal solution, maybe also adding ethanol as found in the literature. Another possibly is continue

to use an inorganic binder but trying to use a different, as the $MgSO_4$ to see if is better, because has the same ions of the electrolyte.

7.2.2 Stack device

For the stack device one improvement could be change the fiber glass with a less thick one, so that the distance between the two electrodes decreases with an increase of the capacitance. The electrodes can be modeled so that they can directly come out by the device without the introduction of the titanium that can create reactions, although are reversible.

7.2.3 Planar device

To correctly characterize a planar device is necessary transform one electrode of the device into a reference or pseudo-reference electrode.

To do this one possibility is sputter the platinum on one electrode, covering the other with an hard mask. This last experiment is has already been done in the final part of the work demonstrated that it is possible. However is necessary test if effectively this can work as pseudo-reference and then characterize each electrode with this. Once that the characterization is obtained, is possible repeat the steps followed in this thesis trying to create an asymmetric planar device. In this direction is possible characterize different layouts with different electrode's distance with masks already present.

Another possibility, to save time, is directly test the planar device with a ratio of the areas of 1.6 shown into the mask on the right of the figure 6.1. This because although is needed repeat the characterization, maybe the results are not so different so is possible try to see what happens.

Bibliography

- [1] BengtSundén. «Hydrogen, Batteries and Fuel Cells». In: (2019), pp. 57–79 (cit. on p. 1).
- [2] Martin W. Carlen Thomas Christen. «Theory of Ragone plots». In: 91 (Mar. 2000) (cit. on p. 2).
- [3] Ning Pan Sanliang Zhang. «Supercapacitors Performance Evaluation». In: 5 (2001) (cit. on pp. 1, 5, 6, 14, 19, 20).
- [4] Park, S.-J., Seo, and M.-K. «Interface Science and Composites». In: Volume 18 (2011) (cit. on p. 3).
- [5] B. E. Conway. *Electrochemical Supercapacitors*. New York, USA: Springer, 1999 (cit. on pp. 4, 5, 17, 18).
- [6] L. Zhou, C. Li, X. Liu, Y. Zhu, Y. Wu, and T. van Ree. «Metal oxides in supercapacitors». In: (2018) (cit. on p. 5).
- [7] Nae-LihWu. «Nanocrystalline oxide supercapacitors». In: vol 75 (2002) (cit. on p. 6).
- [8] Patrice Simon and Yury Gogotsi. «Materials for electrochemical capacitors». In: vol 7 (November 2008) (cit. on p. 6).
- [9] Cheng Zhong, Yida Deng, Wenbin Hu, Jinli Qiao, Lei Zhangd, and JiuJun Zhangd. «A review of electrolyte materials and compositions for electrochemical supercapacitors». In: Volume 44 number 21 (2015) (cit. on pp. 6, 21).
- [10] Joana Monteiro Baptistaa, Jagdeep S. Sagub, Upul Wijayantha KGb, and Killian Lobatoa. «State of the art materials for high power and high energy supercapacitors: Performance metrics and obstacles for the transition from lab to industrial scale A critical approach». In: 374 (2019), pp. 1153–1179 (cit. on p. 6).
- [11] Nitin Choudhary, Chao Li, Julian Moore, Narasimha Nagaiah, Lei Zhai, Yeonwoong Jung, and Jayan Thomas. «Asymmetric Supercapacitor Electrodes and Devices». In: 29 (2017) (cit. on p. 6).

- [12] Qunting Qu, Peng Zhang, Bin Wang, Yuhui Chen, Shu Tian, Yuping Wu, and Rudolf Holze. «Electrochemical Performance of MnO₂ Nanorods in Neutral Aqueous Electrolytes as a Cathode for Asymmetric Supercapacitors». In: 113 (2009), p. 14020–14027 (cit. on p. 7).
- [13] Narendran Sekar and Ramaraja P Ramasamy. «Electrochemical Impedance Spectroscopy for Microbial Fuel Cell Characterization». In: (November 2014) (cit. on p. 9).
- [14] Farhad Pargar¹, Hristo Kolev, Dessi A. Koleva, and Klaas van Breugel. «Microstructure, surface chemistry and electrochemical response of Ag|AgCl sensors in alkaline media». In: 53 (February 2014) (cit. on pp. 13, 23).
- [15] W. Wang¹, X. Wei¹, D. Choi¹, X. Lu, G. Yang, and C. Sun. *Electrochemical cells for medium and large scale energy storage: fundamentals*. Elsevier Ltd., 2015 (cit. on p. 14).
- [16] P. L. Taberna. «Electrochemical Characteristics and Impedance Spectroscopy Studies of Carbon-Carbon Supercapacitors». In: vol 150 (2003) (cit. on p. 19).
- [17] Bryan C. Huayhuas Chipana and Juan Carlos Morales Gomero. «Nanostructured Screen-Printed Electrodes Modified with Self-Assembled Monolayers for Determination of Metronidazole in Different Matrices». In: 113 (September 2014) (cit. on p. 22).
- [18] K.W. Vogt, P.A. Hohl, W.B. Carter, R.A. Bell, and L.A. Bottomley. «Characterization of thin oxide adhesion layers on gold: resistivity, morphology, and composition». In: (1993) (cit. on p. 24).
- [19] Amjid Rafique, Usman Zubair, Mara Serrapede, Marco Fontana, Stefano Bianco, Paola Rivolo, Candido F. Pirri, and Andrea Lamberti. «Binder Free and Flexible Asymmetric Supercapacitor Exploiting Mn₃O₄ and MoS₂ Nanoflakes on Carbon Fibers». In: (2020) (cit. on p. 37).
- [20] Maheshwar Shrestha, Ishop Amatya, Keliang Wang, Bocong Zheng, Zhengrong Gu, and Qi Hua Fan. «Electrophoretic deposition of activated carbon YP-50 with ethylcellulose binders for supercapacitor electrodes». In: vol 13 (2007) (cit. on pp. 45, 47).
- [21] Mohammad Mahmudul Huq, Chien-Te Hsieh, and Chia-Yin Ho. «Preparation of carbon nanotube-activated carbon hybrid electrodes by electrophoretic deposition for supercapacitor applications». In: vol 62 (2015) (cit. on pp. 45, 47).
- [22] Arpana Agrawala and Gyu-Chul Yib. *Sample pretreatment with graphene materials*. Comprehensive Analytical Chemistry, Volume 91, 2020 (cit. on p. 46).

BIBLIOGRAPHY

- [23] A Zyglar, M Slominska, and J Namiesnik. *Soxhlet Extraction and New Developments Such as Soxtec*. Elsevier, 2012 (cit. on p. 46).
- [24] *Activated Carbon Kuraray YP50F*. Kuraray (cit. on p. 54).
- [25] *TIMCAL SUPER C65 Conductive Carbon Black Powder*. Cambridge Energy Solutions (cit. on p. 54).
- [26] Caiwei Shen, Sixing Xu, Yingxi Xie, Mohan Sanghadasa, Xiaohong Wang, and Liwei Lin. «A Review of On-Chip Micro Supercapacitors for Integrated Self-Powering Systems». In: (October 2017) (cit. on pp. 61, 62).